ICE YACHT DESIGN

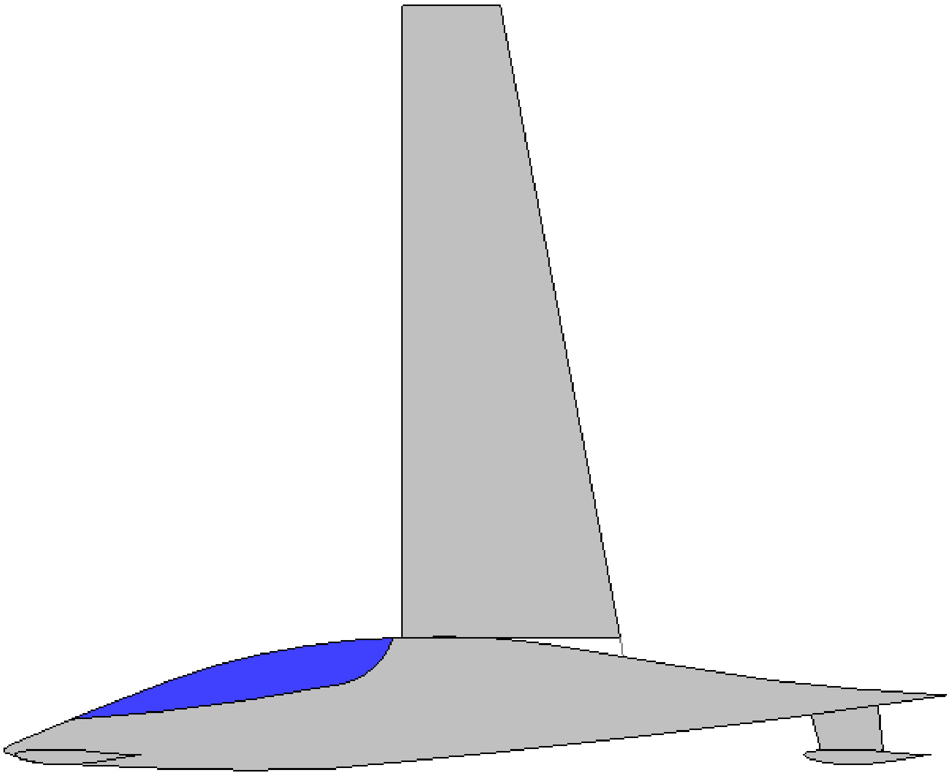

Javier Cuadriello Rodríguez
Imperial College
Aeronautics IV
February 2000

INDEX

1. INTRODUCTION

The objective of this project is to design an ice yacht. We chose to design a high performance one for racing. There are several ice yacht competitions being the DN class the most common. However the designs used for this kind of race haven't evolved in many years. The DN design appeared in 1937 in a competition held by the Detroit News (DN), and it was always designed as low cost vehicle. Using new materials, semi rigid wings allowing for highly efficient airfoil sections and putting a lot of effort in reducing drag by streamlining the body a much higher performance can be achieved. We intended to design the formula one equivalent of an ice yacht. This combines the capacity to travel at high speed but also allows for a certain amount of maneuverability.

Due to time constrains I concentrate mainly in the aerodynamic, stability and geometrical aspect of the design and less in the mechanic part.

2. SPECIFICATIONS

2.1 INITIAL SPECIFICATIONS

- High Performance rigid sail racing ice yacht
- Crew: 1
- Bow Steerer with the runners
- Wing behind pilot
- Single Sail
- 2 Wings
- 5-7 meters long
- Composite frame structure
- Covered Cockpit
- Mechanically Controlled
- Sail options (a) Dyna-wing (b) Composite buckling wing
- Pilot on the back
- Maximum speed at favorable wind conditions: 240 Km/h
- Easily transportable.

2.2 REVISED SPECIFICATIONS

- High Performance rigid sail racing ice yacht
- Crew: 1
- Four runners, from steering.
- Wing behind pilot
- Single Sail
- 4 Wings
- 6 meters long
- Composite frame structure
- Covered Cockpit
- Mechanically Controlled
- Sail options (a) Dyna-wing
- Pilot on the front
- Maximum speed at favorable wind conditions: 240 Kph.

3. DIVISION OF RESPONSABILITIES.

PERFORMANCE

a. Overall Performance: Rhys
b. Longitudinal Stability / Weight / CG: Severin
c. Lateral Stability: Javier
d. Overall Drag: Javier

WING DESIGN

a. Lift / Drag: Javier
b. Skate Wings: Rhys

STRUCTURE

a. Wing: Severin
b. Body: Rhys

MECHANISMS

a. Mast / Sail: Severin
b. Steering / Suspension (front): Javier
c. Suspension (rear): Rhys

GENERAL DRAWINGS

a. Javier

VARIOUS

a. Manufacturing Issues: all
b. Brakes: TBD
c. Transportability: TBD (cancelled)

4. INITIAL PROCESS

In order to find the best general dimensions and general configuration such as number of wings a general initial estimation of the drag and lift was necessary. Some design features and parameters were decided in advance, the main ones are:

- Single Sail.
- Downwards force provided by aerodynamics forces coming from wings.
- Simple single wings.
- Maximum width of 3.5 meters.

Several parameters were tested over an over following the process shown in Appendix A. Results from the initial sizing process can be seen in Table 1A in Appendix A.

This figure shows how the initial overall drag estimation has to be made to see what kind of drag from the wings and body could be tolerated. At this stage we were still considering two main configurations: 1 wing or two wings. This initial sizing process made us change the configuration from the original 1 wings configuration to a 2-wing configuration. This and a few other parameters gave a new set of revised specifications.

This initial process was conducted in parallel by Mr. Severin de Valence and I. The results agreed very well and the initial configuration was chosen.

5.WINGS

5.1 PRINCIPLE

The ice yacht achieves the down force necessary for stability by the negative lift produced by its wings. They must provide enough force to maintain the ice yacht stable at any velocity up to 240 Km/h compensating the lateral force produced by the sail. The runners are also positioned in the wings to provide width for the yacht, which is directly related with lateral stability. The stability of the ice yacht is conditioned to the integrity of the wings. If the wings are damaged and they fail to produce the necessary down force it could lead to a very dangerous situation. That is one of the reasons why the wings produce an excess force throughout the velocity range of the ice yacht. This will be discussed in more detail later.

5.2 WING CONFIGURATIONS

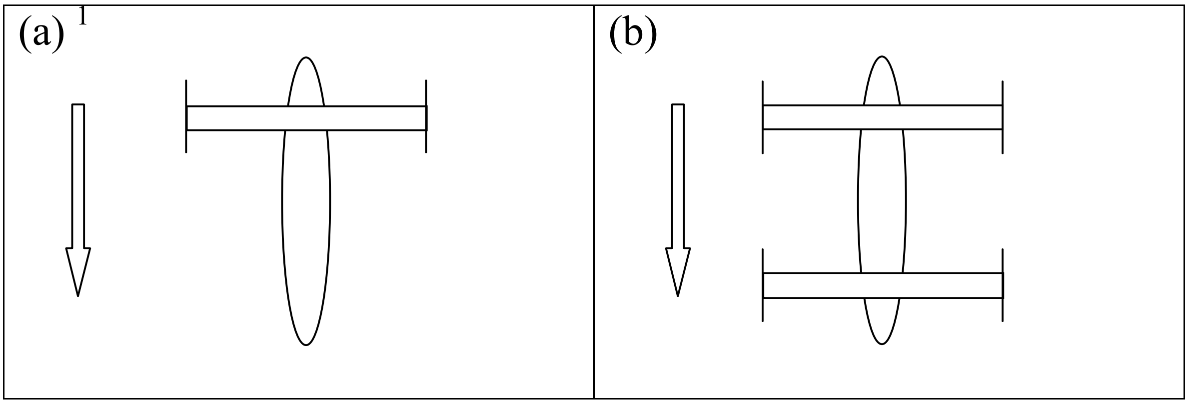

Two configurations where considered, a 2 wing (1 complete wing, Fig A) configuration and a 4 wing (2 complete wings, Fig. B) where considered.

The initial calculations show that 2 wings (Fig B above) provide more stability than 1 (Fig. A above). The weight and down force are also better distributed and most importantly the drag is reduced as the lift coefficient and the cord required to produce the necessary down force at maximum speed create a larger drag. The formula to calculate the drag in the initial calculations was:

$$D = q_{\infty} S \left(Cdo + \frac{Cl^{2}}{\pi \cdot e \cdot AR} \right)$$

C_{do} was initially assumed to be 0.006

---

[1] Arrow indicates direction and sense of advance of the ice yacht, not the wind.

"e" indicates the lift distribution on the wing, I also assume near elliptical distribution i.e. e=1 .
I also had to neglect the influence with the ground and it is hard to quantify its effects.

5.3 WING AIRFOIL SELECTION AND ANGLE OF INCIDENCE.

Selecting the airfoil also involved selecting the angle at which it should operate. Airfoils were selected from the NACA sections described in The Theory of Wing Sections by H.Abbot and A.E. von Doenhoff. The characteristics to look for where:

1. Cl of about 0.7 at a speed of 240 Km/h (Re= 4 million) with minimum drag (Cd ≈0.006).
2. Moderate camber to prevent separation due to proximity of the ground.
3. Acceptable thickness for structural reasons.

In the preliminary airfoil selection some assumptions where made:

1. The effects of aspect ratio where ignored as the variation is small.
2. The effects of the iteration with the ground were neglected due to the difficulty to compute them.
3. A NACA airfoil could give an acceptable performance.

Split flaps were considered but were later dropped, as there were not necessary to achieve the desired lift and drag characteristics.

Airfoils with properties close to those desired were taken form The Theory of Wing Sections[2] and their drag and lift characteristics were compared at 3,4 and 5 degrees of incidence. The candidate airfoils can be found in Table 1B in appendix B.

The selected airfoil was the NACA 63(1)412 with no split flap for its good compromise between drag and lift at the required angles of incidence and it reasonable drag a about 240 Km/h. The shape of this airfoil can be seen in Appendix A below Table 1B.
To decide the optimum angle of incidence the Cl was corrected for aspect ratio using the following formula, the results can be found in table 2-B Appendix B

$$\left(\frac{dCl}{d\alpha}\right)_{for\_AR\_of\_\text{int}\,erestt} = \frac{\left(\frac{dCl}{d\alpha}\right)_{AR=\infty}}{1+\frac{\left(\frac{dCl}{d\alpha}\right)_{AR=\infty}}{\pi \cdot AR_{(of\_\text{int}\,erest)}}}$$

It can be seen in the Cl correction results in Fig 1B in appendix B that the correction causes little effect in the results. Therefore the initial assumption for selection was valid. For better accuracy the corrected Cl results were used from this point.

Three incidences were carefully investigated. Appendix B shows the comparison of Cl (Fig

---

[2] Theory of wing sections Ira H Abbott and Albert Vovn Doenhoff.

4B), Cd (Fig 3B) and L/D (Fig. 2B) of these incidences for the NACA 63(1)412 as speeds increase. These results were calculated using the 2-D wing analysis software XFOIL.
The angles tested were 3,4 and 5 degrees as they were all close to offer the necessary lift and drag characteristics. Bigger angles could create separation when traveling at high speeds close to the ground, and smaller angles couldn't produce enough negative lift to keep the Ice yacht for the whole velocity range.
From the graphs in Appendix B (Fig 2,3,4 B) I chose an incidence of 4 degrees as it offered the best compromise between lift and drag and it provided enough down force to maintain stability for the range of velocities of the yacht
Twin wings or the addition of flaps could have produced better aerodynamic performance. However it is hard to compute the interaction between both wings. Furthermore the wings contain the steering mechanism and support the weight of the yacht. Therefore having a unique thicker wing makes it easier to place the necessary structure, suspension and steering systems.

5.4. WING GEOMETRY AND POSITION.

The wings are positioned at 10 cm from the ground measuring from the point of maximum thickness This is a good compromise between maximizing the increase in down force created by the proximity of the ground and the necessary clearance to prevent the wings from been damages by imperfections in the ice. This 10 cm measure assumes a neutral position of the suspension , defined here as the normal position of the suspension supporting the weight at 200Km/h over a flat surface . Depending on the suspension position they can be 3 cm higher of lower. The leading edges of the 2 wings are 5m apart. As they are inverted the trailing vortex will move up and this distance should allow for a negligible interference between the two. The width of a single wing was limited to 3.5m for structural reasons and the cord was adjusted to provide the necessary down force. The resulting aspect ratio is 5 and a cord of 0.7 meters. For specific information on the position of the wing consult the drawings in Appendix J.

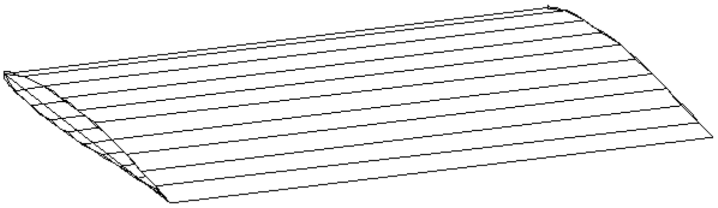

5.5 FLOW OVER THE WING AT DIFFERENT VELOCITIES.

The behavior of the flow over a range of velocities can be observed in Fig. 1C in Appendix C. It can be seen in the different pressures distribution from 17 Km/h to 239 Km/h how the flow behaves better at higher speeds. Abrupt changes in the Cp distribution at the slowest speeds suggest areas of flow separation. However the lifts coefficients obtained provide enough down force to accomplish their task of keeping the yacht stable.
A more detailed analysis of the flow at the maximum speed can also be seen in Fig. 2C appendix C. We can observe how the Cp distribution behaves in a very smooth way, by also looking at the Cf distribution and the boundary layer thickness we can observe that the flow remains always attached. However we can see from the Cf distribution graph how the flow becomes turbulent at about $x/c = 0.2$ in the upper surface (actually lower as the airfoil is inverted) and at $x/c= 0.7$ in the lower surface (actually upper as the airfoil is inverted). At these distances a sudden increase in Cf can be observed due to the turbulent transition.

Furthermore in the third plot an increase in the boundary layer thickness at x/c=2 in the upper surface (lower surface).
Once again these results were calculated using the 2-D wing analysis software XFOIL in the Silicon Graphics and neglect the effects with the ground.

5.6 EFFECT OF THE GROUND.

The air velocity between the airfoil and the ground is increased and the local pressure increased due to the presence of the ground, the streamlines are forced together under the airfoil and the velocity increase. This creates lower pressure that increases the down force of the wing. Due to the small distance between the wings and the ground and the relatively large velocity of the flow it is not possible to make a good approximation of this force. I opted for a more conservative design that doesn't rely in this effect to maintain stability. Therefore the wings provide enough force to keep the ice yacht stable even without this beneficial factor. Any increase in the down force will only add to the safety.
Ideally this flow would be computed either by advance CFD solvers of by wing tunnel testing over a moving floor. This could lead to a reduction in the wing area necessary to maintain stability giving a considerable reduction of the drag.

5.7 SWEEP EFFECTS

The wings themselves have zero sweep, however the ice yacht is exposed not only to the wind speed coming from it displacement (Vs) but also to the true wind (Vt) . Therefore it is "seeing" the resultant velocity from these two, this velocity is called apparent wing (Va) with forms an angle β with Vs. The transverse component of this apparent wing i.e. Vt , can affect the flow over the wind. Looking at the Fig. 1,2,3 E in appendix E we can see how this situation is equivalent to having a forward swept wing in one side and a backward sweep wing in the other. Therefore they are affected by the same kind of issues concerning swept wings.

1. Cp distribution over the wing would be that of a swept wing
2. And any disturbance in the attachment line could affect large part of the wing, this can be very dangerous for this kind of design as it (a) relies on aerodynamics forces from these wings for stability and (b) they wings very close to the grounds and could be hit by small objects on the ice.
3. The cross flow gives a longer effective path over the wing, which gives a thicker boundary layer and increases the risk of separation.
4. Destabilizing cross flow in the boundary layer.

Computing the effect of this cross flow and it effect on the boundary layer is difficult. As the cross flow velocity is small compared with Vs and the "sweep angle" β is very small at high speed, this effect is ignored.

6. LATERAL STABILITY

One of the most important aspects of the design is keeping the yacht stable. "Driving" the ice yacht would be a dangerous sport due to the high speeds and the unpredictable nature of ice. Lateral stability is directly linked to the performance of the wings in this design as they have the task of creating the downward force that keep the yacht stable. In this section I will concentrate in the discussion of the achieved stability at different speeds.

I define “stability margin” as the excess down force produced by the wings. In graph 1D in appendix D it can be seen how this margin decreases slightly with speed. However there is always a considerable safety factor. Furthermore there would be even a higher stability margin if we could compute the increase in down force cause by the presence of the ground.

The formula used in the initial design process to determine the amount of lift necessary to keep stability is shown below. Initial H was assumed and was later calculated more accurately by the person in charge of the sail design.

$$F_{Hperm} \approx L_{Perm} \approx (Weight + Downward\_aerodynamic\_force) \times \frac{B}{H}$$

Where F_{hperm} is the permissible heeling force, W is the Weight , B is the semi-span of one of the wings and H is the height of the center of effort of the sail.

7. BODY DESIGN AND BODY DRAG

7.1 BODY SHAPE

The body shape was inspired in the Morelli Basic body Shape.[3] This kind of shape was created to provide a minimum drag and maximum downwards force as well as giving enough thickness to make it suitable for car bodies. The cross sectional area was kept at minimum to minimize drag. The pilot position is as low as possible ad he/she doesn’t enjoy much interior space. This is a high performance racing vehicle and pilot comfort is not a primary aspect. He/She has enough space to move the controls. The body shape, helped by the presence of the ground should create a downwards force, I assume that this force will compensate for the missing lift force in the forward wing due to the presence of the body.

7.2 BODY DRAG CALCULATIONS

In order to find an approximation to the drag (and lift) generated by the body I used a program called *MicroTunnel* , written by Axel Rohde. Ideally wind tunnel testing and 3-D CFD solvers should be used, however I didn’t have necessary resources or time to run wind tunnel tests or the computer power and time to perform complex computations around the ice yacht.
Microtunnel is a compressible CFD solver. We are not particularly concerned about compressibility for the estimation of the body drag, however the program can only consider compressible flow, making it very slow.

The author of the program was contacted to obtain information on the algorithm used and the computing power required. According with him for a test with a characteristic length of 10 m, for Mach = 0.1 at sea level, i.e. 34m/s, the simulation Stop Time should be about 5 seconds. Since S = V *T = 34m/s * 5s = 170m, thus the tested shape will have traveled about 17 Ch.L., which is plenty for the flow field to converge. The problem has to be scaled to a Ch.L = 1m and T = 0.5s, since a Stop Time of greater than 1s is not be accepted by the program. The result is the same, since MicroTunnel is an inviscid flow solver, i.e. actual length scale does not matter in the computation (thus no Re # input).

---

[3] Morelli, Alberto, “Aerodynamic Basic Bodies Suitable for automotive Applications, ” Proceedings of the First Symposium on Road Vehicle Design, Special Publication SP3, 1983.

In a 200MHz Pentium at a resolution of 200x150, and the entire test (until convergence is reached at T = 0.5s sim-time) would take about 500 minutes, or 8.5hours to compute. Every time the tunnel resolution is doubled, CPU time increases by a factor of 8, because the computer has 4 times the amount of work to do (twice in X, and twice in Y), and the integration time step gets halved due to stability requirements. Thus at 400x300 resolution the computation would take 67 hours, and at 800x600 it would take 22 days on a 200Mhz Pentium. On a 800MHz Pentium III, the above computation times would be one fourth, or less. Thus a 800x600 test in about 5 days

For the actual test for the Ice Yacht body I could only tested for the maximum speed, i.e. 240 Km/h. Ideally I could have tested it for different velocities but the computation time didn't allow more tests. For the body the characteristic length is 6m, and the cruising speed is 66m/s. I assume that only 10 characteristic lengths are enough for the flow to converge. According with this the stop time used for the test was 1s. Scaled to 0.1 and characteristic length of 1.

The tests where performed on a PIII450 with 64Mb of RAM. The main test for the side shape took approximately twelve hours to complete and eight hours for the top view of the body.

The input parameters used where:

WIND TUNNEL RESOLUTION = 300 x 225
FLOW MACH NUMBER, M = 0.19
ANGLE OF ATTACK (deg) = 0
STATIC PRESSURE (hPA) = 1015
STATIC TEMPERATURE (K) = 273
CHARACTERISTIC LENGTH (m) , L = 1.00
GAS CONSTANT (J/Kg-K) , R=287
SPECIFIC HEATS RATIO, k=1.40
TIME STEP (ms) , dt = 2.00
STOP TIME (S) , T = 0.200

Governing Equations

Microtunnel is based on the 2-D unsteady Euler equations of invisid flow, a system of integral conservation equations for mass, momentum, and energy. These can be written in vector notation as the sum of an area and line integral.

$$\frac{\partial}{\partial t}\int_{cell} QdA + \oint_{\partial Cell} FdS = 0$$

Where

$$Q = \begin{bmatrix} \rho \\ \rho u \\ \rho v \\ \rho e_0 \end{bmatrix}, \; F = \begin{bmatrix} \rho v_n \\ \rho u v_n + p \cdot n_x \\ \rho v v_n + p \cdot n_y \\ \rho h_0 v_n \end{bmatrix}$$

The velocity across a cell boundary is simply defined as the dot product of local velocity vector and outward unit normal vector to the boundary.

$$v_n = v \cdot \hat{n} = \begin{pmatrix} u \\ v \end{pmatrix} \cdot \begin{pmatrix} n_x \\ n_y \end{pmatrix}$$

The stagnation energy and enthalpy are the sum of static and dynamics parts, respectively.

$$e_0 = e + \frac{1}{2}\left(u^2 + v^2\right)$$

$$h_0 = h + \frac{1}{2}\left(u^2 + v^2\right)$$

For a calorically perfect gas, the specific heats for constant volume and the constant pressure processes, Cp and Cv, as well as the ratio γ and difference R can be assumed constant.

$$\gamma = \frac{Cp}{Cv}$$

$$R = Cp - Cv$$

Pressure, density, and temperature are related by the perfect gas law. For a perfect gas, the speed of sound is only a function of temperature.

$$p = \rho \cdot R \cdot T$$

$$a^2 = \gamma RT$$

With the above constitutive relations, the system of integral conservation equations is now closed. We have four equations for four unknowns: Two velocity components and two thermodynamic state variables, such as pressure and temperature. The steady-state solution to the flow field is obtained by marching in time from an initial condition of uniform flow subject to two sets of boundary conditions: uniform flow at far field, and tangential flow with zero energy flux at the body's surface. The explicit integration routine employs Van Leer's flux vector splitting technique.

Vector Flux Splitting

For a given local Mach number $M_n = v_n / a$, normal to the cell boundary, the flow vector $\vec{Q}$ and flux vector $\vec{F}$ can be written in the following format, after expressing energy, enthalpy, and pressure in terms of the local speed of sound,

$$\vec{Q} = \rho \cdot \begin{bmatrix} 1 \\ u \\ v \\ \dfrac{a^2}{\gamma(\gamma-1)} + \dfrac{u^2+v^2}{2} \end{bmatrix} \qquad \vec{F} = \rho \cdot a \cdot \begin{bmatrix} M_n \\ u \cdot M_n + \dfrac{a}{\gamma} \cdot n_x \\ v \cdot M_n + \dfrac{a}{\gamma} \cdot n_y \\ \left(\dfrac{a^2}{(\gamma-1)} + \dfrac{u^2+v^2}{2}\right) \cdot M_n \end{bmatrix}$$

In a central difference type scheme, the flux $\vec{F}$ is split symmetrically into right and left running fluxes, $\vec{F}^{+}$ and $\vec{F}^{-}$, respectively,

$$\vec{F}^{\pm} = \frac{1}{2} \cdot \vec{F}$$

A central difference type flux split scheme does not take into consideration the direction of signal propagation within flow field and therefore cannot distinguish between subsonic and supersonic flow. As a result, shock waves cannot be properly resolved, and spurious oscillations within the flow field are common, even for purely subsonic flows.
Based on an eigenvalue analysis of the Euler equations , Bram Van Leer proposed an upwind scheme which splits the flux $\vec{F}$ according to the locally characteristic directions. Van Leer's scheme clearly separates subsonic from supersonic flow depending on the local Mach number.

If $M_n \leq -1$, then

$$\begin{aligned} F^{+} &= 0 \\ F^{-} &= F \end{aligned}$$

If $-1 < M_n < 1$, then

$$F_1^{\pm} = \pm \frac{\rho \cdot a \cdot (M_n \pm 1)^2}{4}$$

$$F_2^{\pm} = F_1^{\pm} \left(\frac{n_x (\pm 2a - v_n)}{\gamma} + u \right)$$

$$F_3^{\pm} = F_1^{\pm} \left(\frac{n_y (\pm 2a - v_n)}{\gamma} + v \right)$$

$$F_4^{\pm} = F_1^{\pm} \left(\frac{a^2}{\gamma - 1} - \frac{(\pm a - v_n)^2}{\gamma + 1} + \frac{u^2 + v^2}{2} \right)$$

If $M_n \geq +1$, then

$$\begin{aligned} F^{+} &= F \\ F^{-} &= 0 \end{aligned}$$

A derivation of the above result can be found in the following reference: Meng-Sing Liou, Bram Van Leer, and Jian-Shun Shuen, "Splitting of Invisid Fluxes for Real Gases" NASA Technical Memorandum 100856, April 1988.

The test was run on the 2D shape of the body from the top and from the side and from the top and the results for the Cd were averaged.
The relevant results given by the program are:

Cl = -0.210
Cd (average between tests) =0.1355

The results can showing the velocity and pressure distribution and the stream lines around the body in isolation can be observed in Appendix F and the development of the flow around the body can be founds in the CD accompanying this report. The graphs and results show that the body has very good aerodynamics properties and creates a low drag coefficient as well as some downwards lift. In order to optimize the boy shape the program should be run several times trying different possibilities.

Validity of results:

There are a series of important assumptions and neglected factors in this test. The main one is the fact that the test ignores the presence of the ground. This should make the lift coefficient even smaller (negative value, absolute value bigger). As this is only a beneficial factor neglecting it just leads to a more conservative design.
Furthermore the tests assume that the body is 2D and neglect the influence of the interaction with the main sail and wings.

8. OVER ALL DRAG

The results for the detailed drag calculation can be seen in Appendix H. Table 1H in this appendix shows the different drag forces produced by different component in a range of speeds. Fig 1H shows how much "thrust" or forward force produced by the sail there is exceeding the drag force. The ice yacht will accelerate as long as this difference is positive. Therefore it can be seen in Fig. 1H that the maximum possible velocity is 234.65 Km/h, that is the point where the line cuts the X-axis. This is not the 240 km/h specified but is very close. Further optimization of the body shape and operational angle of incidence of the wings and the sail as well as the reduction of the drag from the sail if we could calculate the effects with the grounds and adjust their area, could easily take us to 240Km/h.

9. HUMAN FACTORS AND ERGONOMICS

The forward part of the body of the ice yacht was created such that it could accommodate a range of pilot sizes. I used the Def Stan 00-970 specification for pilot sizes (See appendix G), these are used for military aircraft but I use them in the ice yacht as they provide a comprehensive reference of human dimensions for a 99% of the population.
The steering wheel was placed I (See Appendix J - Drawings) in a position where even the smallest pilot could reach it and it is not uncomfortable for a bigger pilot.
As mentioned before , in order to keep the cross sectional area as small as possible the pilot doesn't enjoy of much internal space.

10. STEERING & FORWARD SUSPENSION

10.1 STEERING

Steering and suspension systems can be an extremely complex problem and its design could be de subject for a complete project.
There are three main kinds of steering systems , these can be seen in the diagram below. However in most cases the steering system is a mix between on the "pure" systems in the diagram.

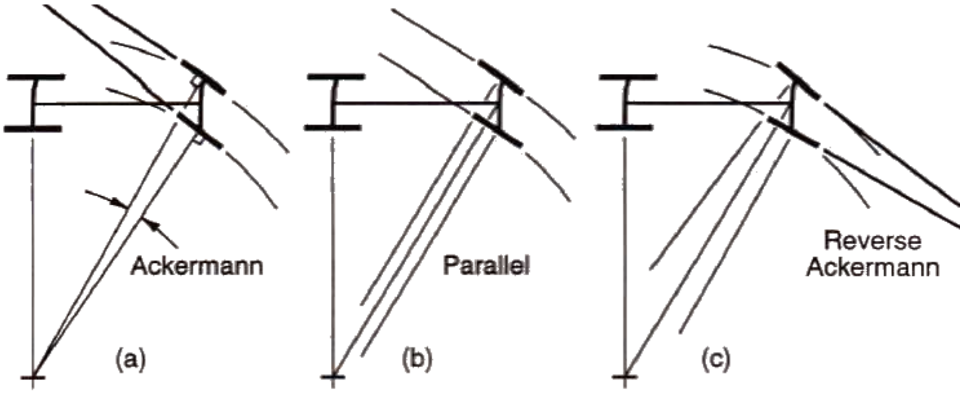

(a) Ackermann, (b) parallel, and (c) reverse Ackermann steering.

I chose an almost parallel steering for its simplicity and because it could be made with a smaller number of parts .I assume that the ice yacht is going to turn at relatively low speeds. For stability reasons and due to the fact that it has to adjust its sail to the new wind direction after the turn, high speed turning is probably not a good idea. Initially in the design process we decided that this kind of ice yacht would race in a large triangular circuit with sides between one and two kilometers. Therefore it only has to turn three times every lap and low speed turning is acceptable.

10.2 FORWARD SUSPENSION

The suspension of the ice yacht is a very important factor. Cars have wheels that provide a considerable amount of suspension, however we only have metal blades. Furthermore we are moving in an unprepared surface. Forward suspension is particularly important as it meets all the imperfections in the ice, the backward runner move on the trail of the forward runner and this makes the path relatively easier for them. I allow the forward runner to pivot freely (with limits, see drawings, Appendix J, and damping incorporated in the hinge) to allow them to follow the floor more easily. The runners are supported by a coil spring shock absorber. As there was not time to design the shock absorber in detail, I assume that it has an inside damper, i.e. a co-cylindrical systems consisting in a damper surrounded by a coil spring absorber.
At normal equilibrium position the wing should be at 10 cm from the flow from the closes point in the airfoil. Equilibrium position is defined here as the position of the suspension when traveling in a perfectly flat surface at a speed of 200 Km/h. It can retract 3.2 cm more and extend 3cm more, i.e. the whole range is 6 cm.
The suspension systems are below the steering systems and it moves completely with the runner when it is steered.
As it can be seen in the drawing all the suspension is covered to minimize parasite drag.

Specific dimensions of the suspension steering components as well as detailed analysis of the damping and vibration modes could not be performed due to the limited amount of time and the complexity of the task. As mentioned before the main emphasis of this project was put into the aerodynamics factors. The suspension and steering systems are only in a conceptual stage.

11. FINAL CONFIGURATION

Appendix I shows a table with the main parameters of the final design. Drawing of the ice yacht with dimensions can be found immediately after in Appendix J.

12. REFERENCES

BOOKS

1. *Aerospace Vehicle Design Notes*, Dr. V.C Serghides, Imperial College 1999
2. Anderson, J.D.; *Introduction to Flight*, McGraw-Hill, Singapore, 1989
3. Marchaj, C.A.; *Aero-Hydrodynamics of Sailing*, Adland Coles Nautical, London, 1991
4. Milliken, W.F. and D.L.; *Race Car Vehicle Dynamics*, SAE International, Warrendale, 1995
5. *Wing Design Notes*, Dr. D. Doorly, Imperial College 1999

INTERNET

1. Dynawing Home Page www.dynawing.com
2. Microtunnel homepage http://www.cfd4pc.com/
3. www1.iwvisp.com/jholtrop/Articles/rigid.htm
4. Tom Speer Website http://home1.gte.net/tspeer/
5. Airfoil database http://www.nasg.com/afdb/index-e.phtml
6. RAFT website http://www.dcaonline.com/raft/

ADVICE

Axel Rohde. Author of *Microtunnel*.
Robert L. Hobbs, DynaWing Co.

APPENDICES

APPENDIX A

DESIGN PROCESS AND PRELIMINARY ESTIMATIONS

ICE YACHT INITIAL DESIGN PROCESS

Fig.1 A

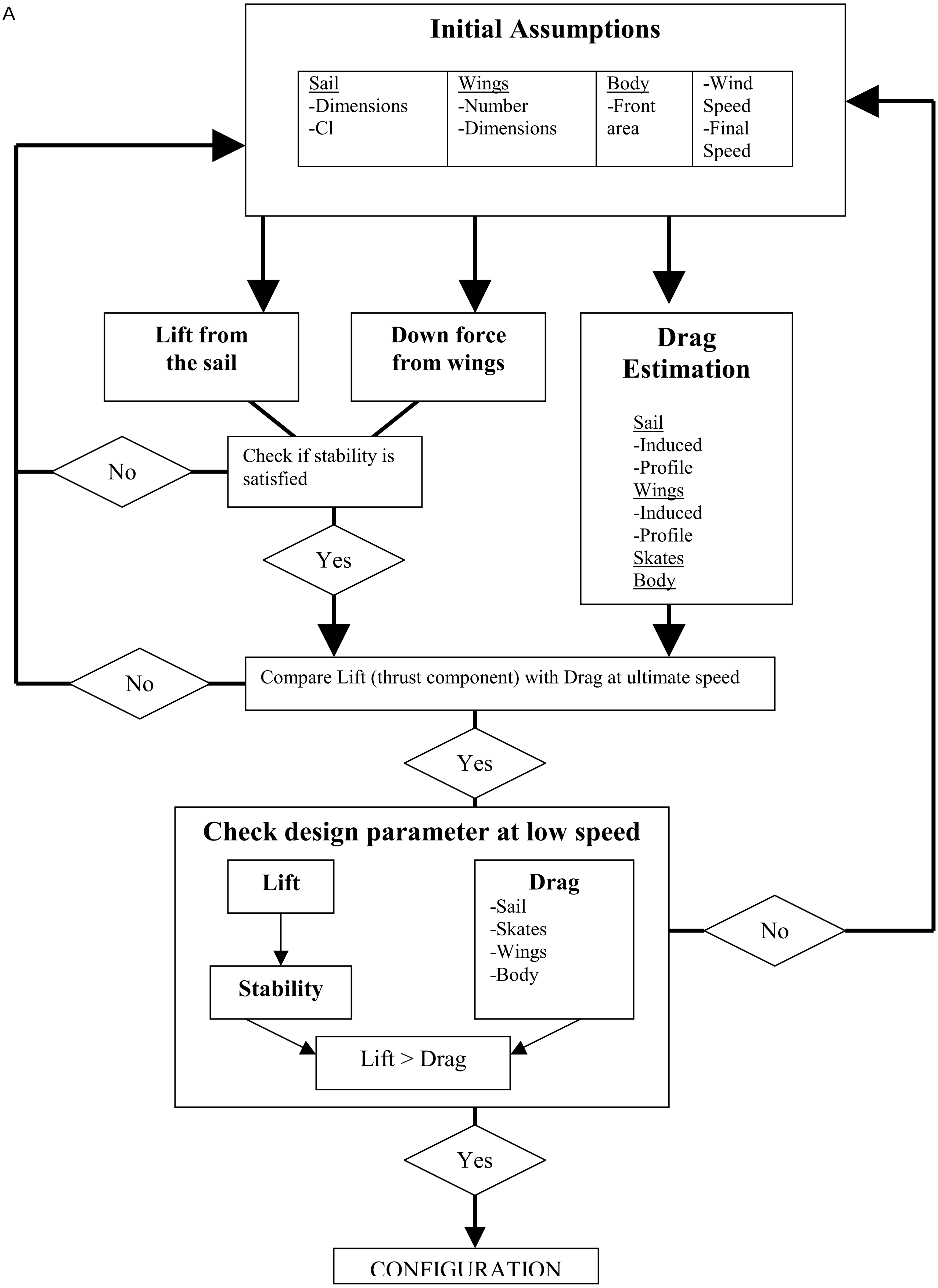

Table 1 A

INITIAL PROCESS

color code

assumed or fixed values

calculated values

INITIAL ASSUMPTIONS

sail dimensions			general parameters				other		
height	4		wind speed	30	8.33333333	m/s	Weight of ice yacht=	210	Kg
cord	1		desired velocity	270	75	m/s	fuselage frontal area	0.3	m^2
Cl	1		density of air	1.295			Parasite Area	0.122651	m^2
Cd0 sail	0.004		viscosity of air	1.72E-05					
Area	4	m^2							
height of pressure coefficient	2	m^2							
L/D	9								
L/D sail	110								

SAIL LIFT

beta= 0.110657 rad
0.001931 deg

Va= 75.46154 m/s

Re for main Sail 4.27E+08

Lift = 14748.611 N
1504.960 Kg

1 WING

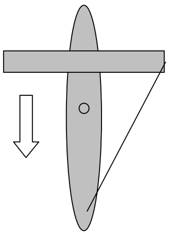

Span (total)	3.5
cord	1.00
distance from nose to cg	4
length of ice yacht	6
Cl of airfoil section	-1.5
Cd0 of airfoil	0.006
distance l.e wing to nose	5
wing distance from the ground	0.1
AR	3.50
dist cg to roll axis	1.32
area of wing	3.50
Re	5.67E+06

Total Down Force Necessary	2163.174	Kg
Aerodynamic Down Force necessary	1953.174	Kg
Aerodynamic down force produced	-19141.104	N
	-1953.174	Kg
stable?	0.000	

color code

stable

unstable

$$D = q_{\infty} S(Cdo + \phi \cdot \frac{Cl^{2}}{\pi \cdot e \cdot AR}$$

e= 1

Drag **2690.4447** N
274.5351748 Kg

2 WING

assumed 20Kg added mass for extra wing

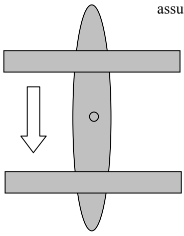

Span (total)	3.5
cord	0.8
distance from nose to cg	2.5
length of ice yacht	5
Cl of airfoil section	-0.710844
Cd0 of airfoil	0.006
distance l.e wing to nose	-
1st wing dist. from the ground	0.1
2nd wing dist. from the ground	0.1
AR wings (each)	4.375
area of 1 wing	2.8
total wing area	5.6
Re	4.53E+06

Total Down Force Necessary	1709.4349	Kg
Aerodynamic Down Force necessary	1479.435	Kg
Aerodynamic down force produced	-14498.56	N
	-1479.445	Kg
stable?	-0.01	

color code

stable

unstable

$$D = q_{\infty} S(Cdo + \phi \cdot \frac{Cl^{2}}{\pi \cdot e \cdot AR}$$

e= 1

Drag **872.2225** N
89.0022984 Kg

Common Drag

Skates
0 N
0 Kg

Body
163.89844 N
16.72433 Kg

assumed Cd 0.15

Main Sail Drag
133.25822 N
13.583917 Kg

assumed Cd 1

Parasite Drag
452.23412 N
46.146339 Kg

1 WING			2 WING		
Wing Drag	274.5351748	Kg	Wing Drag	89.0022984	Kg
Total Drag	3439.699654	N	Total Drag	1621.477465	N
	350.9897606	Kg		165.4568842	Kg
L/D	4.287761315		L/D	9.095785435	

Thrust vs. Drag			Thrust vs. Drag		
thrust	166.1950645	Kg	thrust	166.1950645	Kg
drag	350.9897606	Kg	drag	165.4568842	Kg

thrust must be bigger (or idealy equal) to drag at this speed

APPENDIX B

WING AIRFOIL AND ANGLE OF ATTACK SELECTION

AIRFOIL SELECTION

Table 1 B

WING AIRFOIL CANDIDATES

AIRFOIL NAME	CL	CD	ANGLE
NACA 747A415	0.8	0.006	0.55
	0.7	0.006	0.55
	0.9	0.007	6
NACA 747A315	0.8	0.0079	6
	0.7	0.006	6
	0.9	0.0065	8
NACA 66(3)418	0.8	0.006	5
	0.9	0.0075	7
	0.7	0.005	4
NACA 65(4)421 CLEAN	0.7	0.006	3.5
	0.8	0.006	6.5
	0.9	0.006	6.9
NACA 65(4)421 FLAP	0.7	0.006	3
	0.8	0.006	4
	0.9	0.006	5
NACA 65(4)221 FLAP	0.7	0.006	5.5
	0.8	0.006	7
	0.9	0.006	8
NACA 65(4)221 CLEAN	0.7	0.006	3
	0.8	0.006	3.5
	0.9	0.006	4
NACA 63(1)-412	0.7	0.006	3
	0.8	0.007	4
	0.9	-	-
NACA 63(2)415	0.7	0.006	3
	0.8	0.007	4
	0.9	0.008	5

SELECTED AIRFOIL

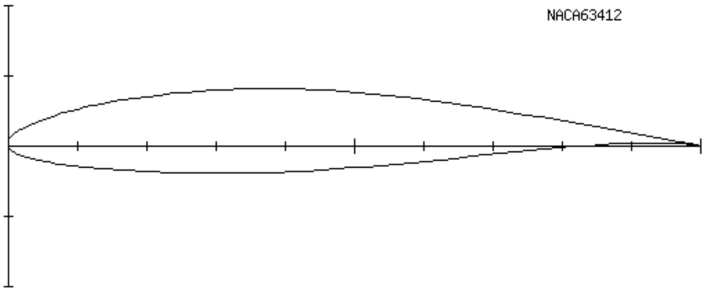

NACA 63(1)-412

LIFT COEFFICIENT CORRECTION
FOR FINITE ASPECT RATIO

Table 2 B

UNCORRECTED CL

Speed (Km/h)	Re	Cl at Angle			
		-2 deg.	3 deg.	4 deg.	5 deg.
17.93	3.00E+05	0.1136	0.6605	0.7608	0.9159
35.86	6.00E+05	0.1148	0.681	0.7896	0.9159
59.77	1.00E+06	0.1157	0.6874	0.7965	0.891
179.3	3.00E+06	0.1192	0.692	0.7943	0.8988
239.1	4.00E+06	0.12	0.6903	0.7947	0.9017

CORRECTED CL

Speed (Km/h)	Re	Cl at Angle			
		-2 deg.	3 deg.	4 deg.	5 deg.
17.93	3.00E+05	0.1099	0.6664	0.7777	0.889
35.86	6.00E+05	0.1152	0.6796	0.7925	0.9054
59.77	1.00E+06	0.1207	0.6762	0.7873	0.8984
179.3	3.00E+06	0.1237	0.6797	0.7909	0.9021
239.1	4.00E+06	0.1238	0.6803	0.7916	0.9029

Fig 1 B

CL VS ALPHA RE=3E5

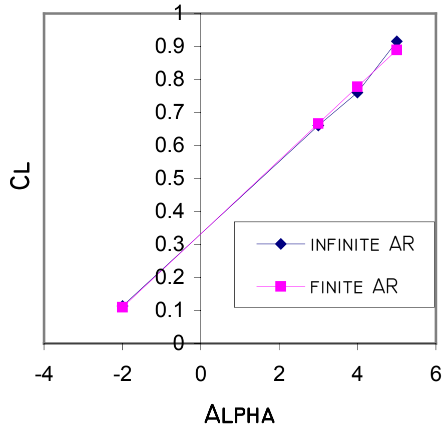

CL VS ALPHA RE=6E5

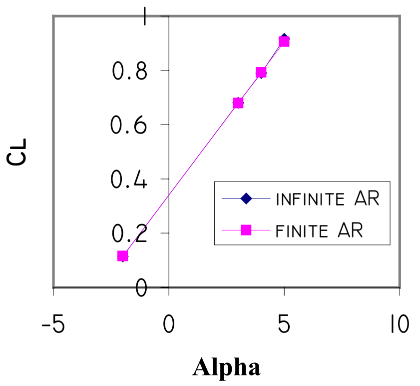

CL VS ALPHA RE=lE6

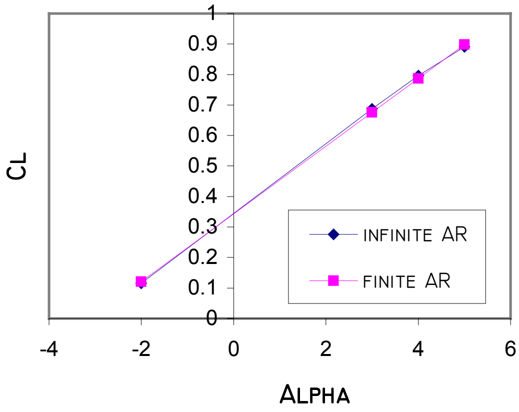

CL VS ALPHA RE=3E6

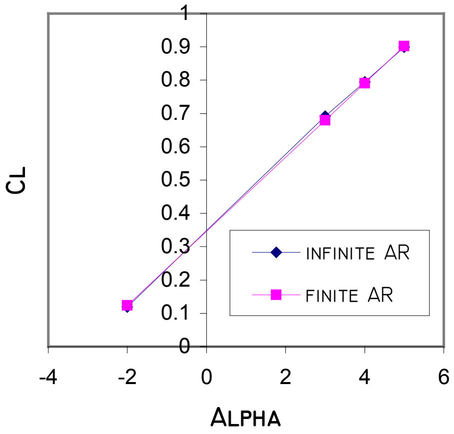

CL VS ALPHA RE=4E6

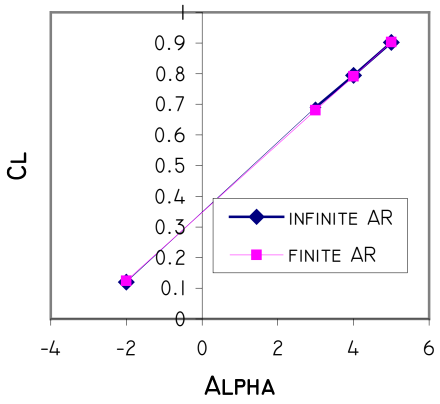

$$\left(\frac{dCl}{d\alpha}\right)_{for\_AR\_of\_int\, erestt} = \frac{\left(\frac{dCl}{d\alpha}\right)_{AR=\infty}}{1+\frac{\left(\frac{dCl}{d\alpha}\right)_{AR=\infty}}{\pi\cdot AR_{(of\_int\, erest)}}}$$

Fig. 2 B

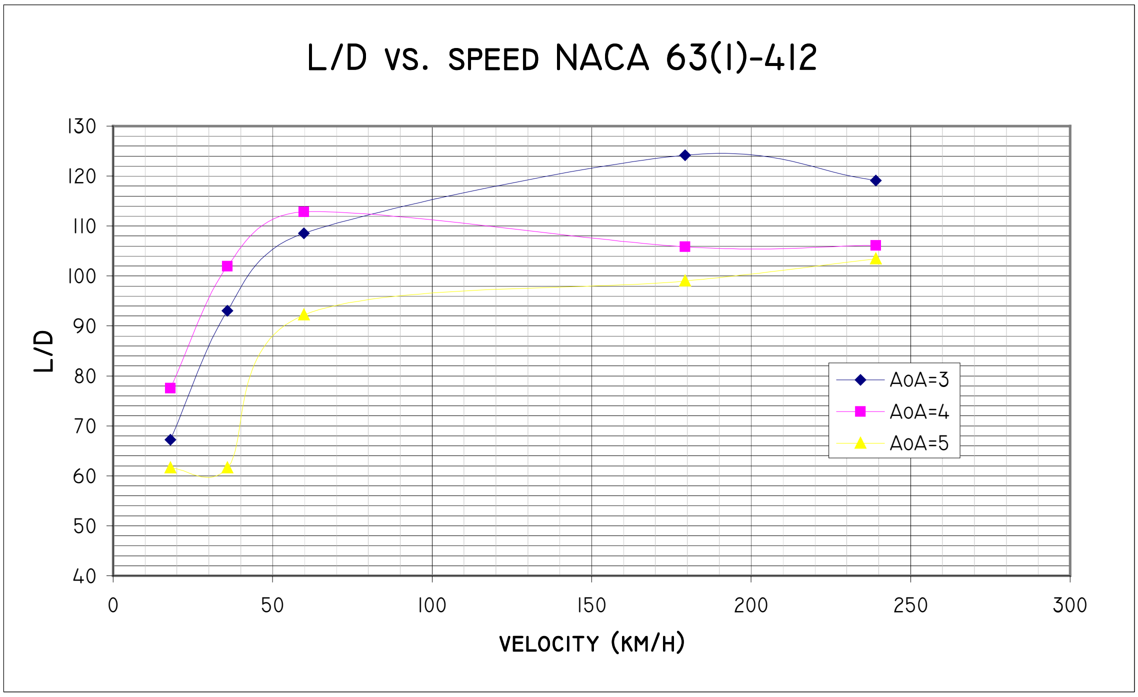

Fig .3 B

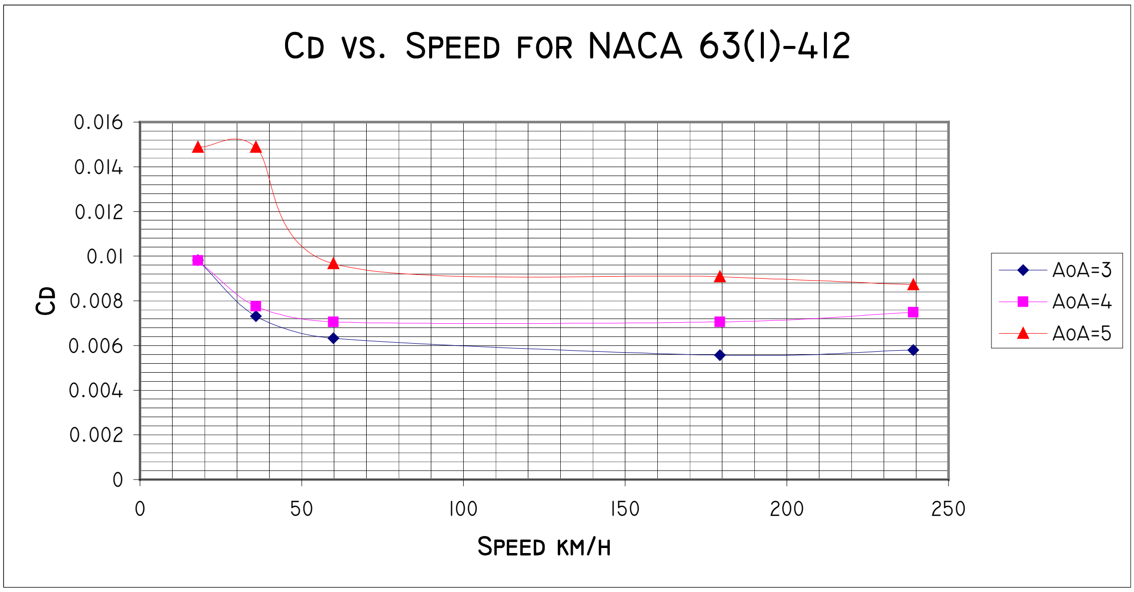

Fig. 4 B

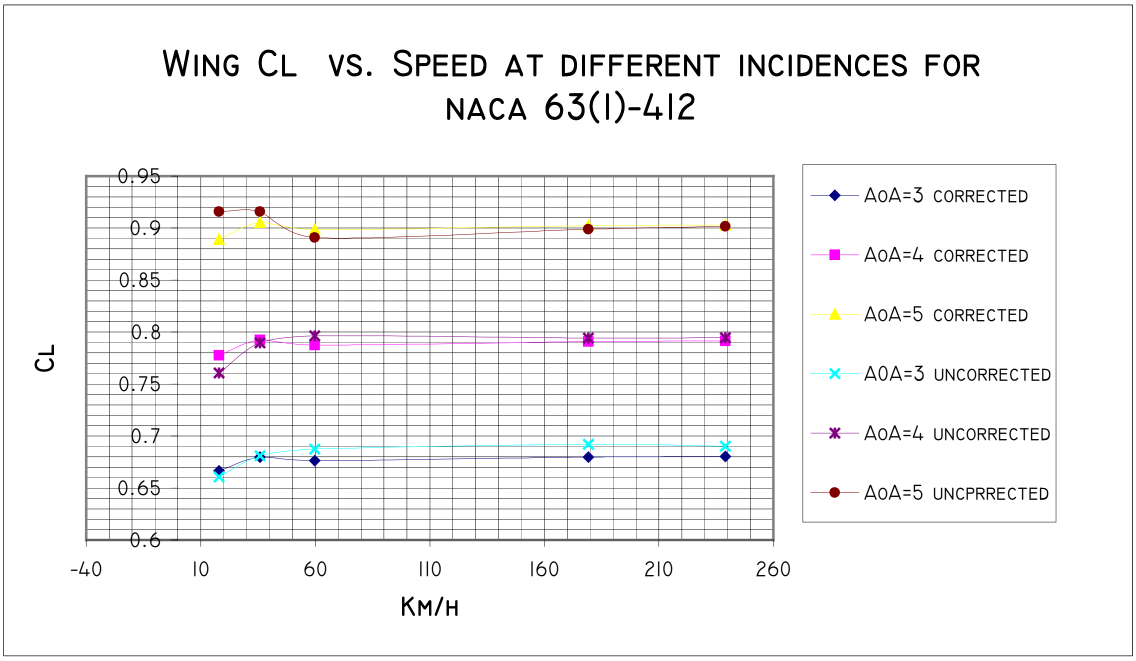

APPENDIX C
WING AERODYNAMICS

Fig. 1 C

CP DISTRIBUTIONS AT DIFFERENT SPEEDS

V=17Km/h

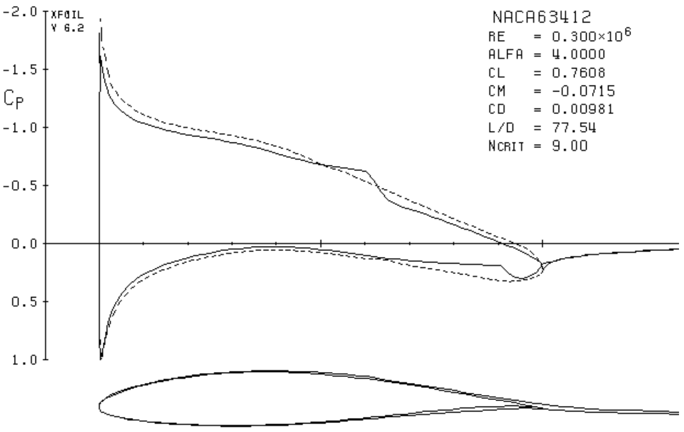

V=35.86 Km/h

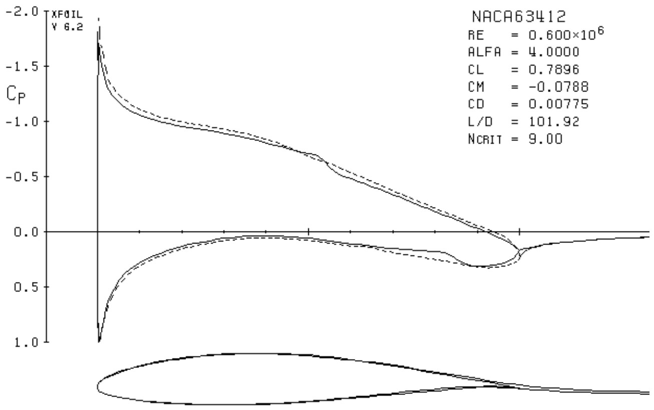

V=59.7 Km/h

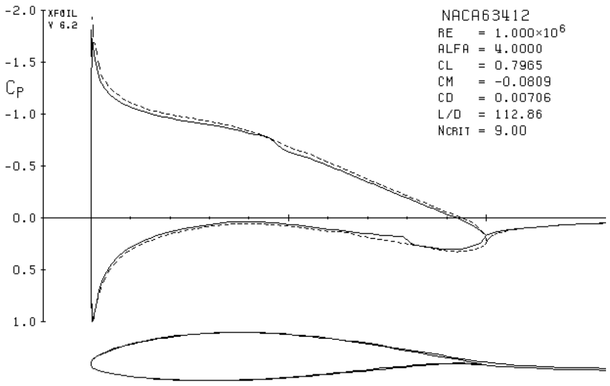

V=179.3 Km/h

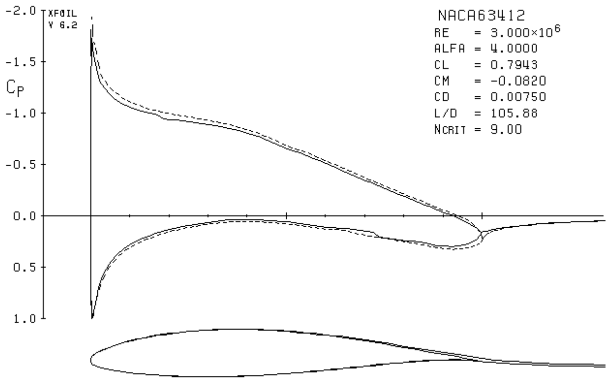

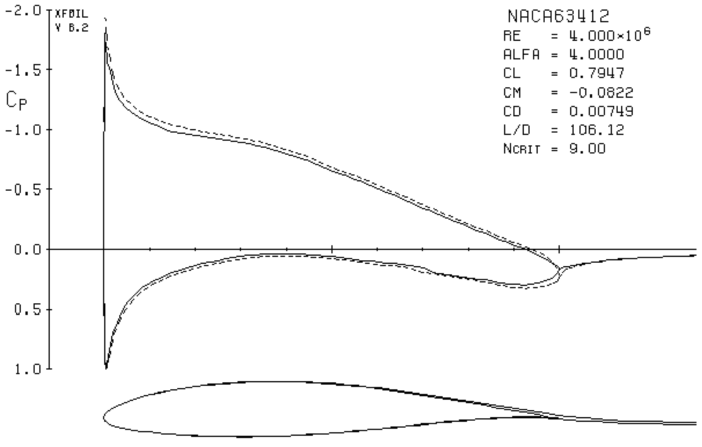

V=239Km/h

Fig. 2 C

CP DISTRIBUTION

MAXIMUM SPEED
RE = 4E06

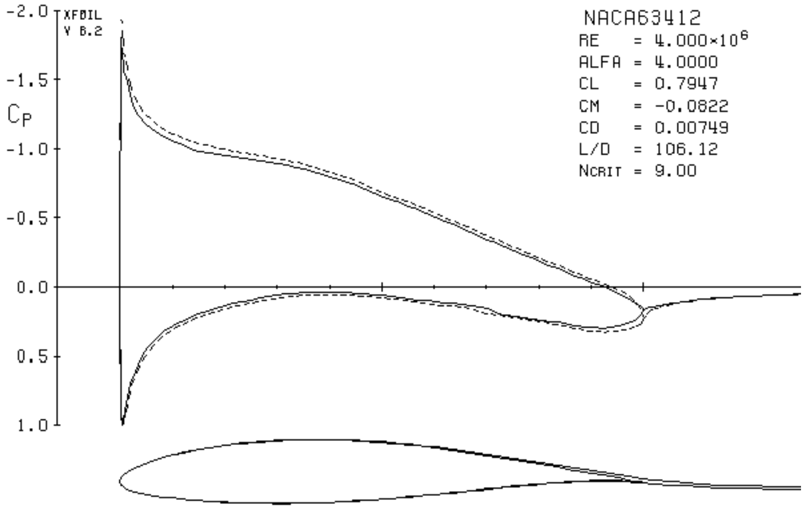

CF VS X/C

MAXIMUM SPEED
RE = 4E06

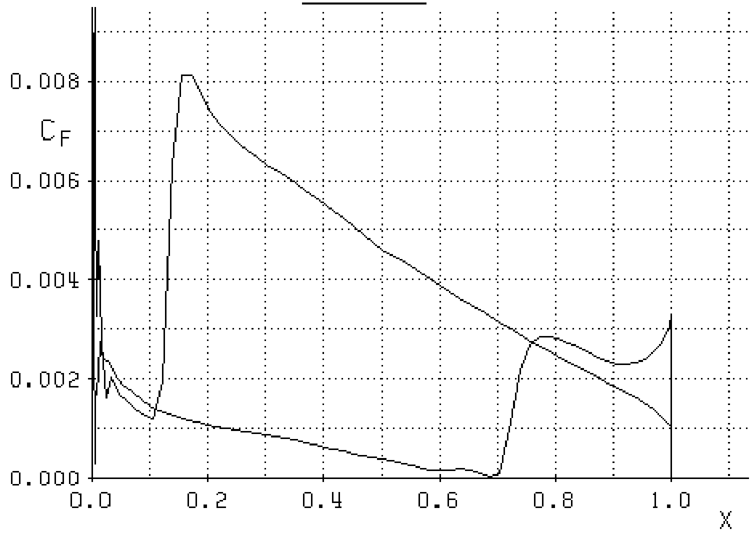

MOMENTUN THICKNESS AND DISPLACEMENT THICKNESS VS. X/C

MAXIMUM SPEED
RE = 4E06

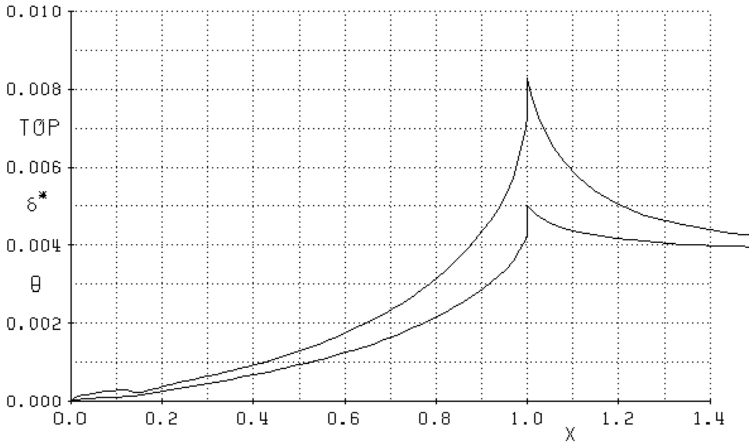

APPENDIX D
LATERAL STABILITY

Graph 1 D

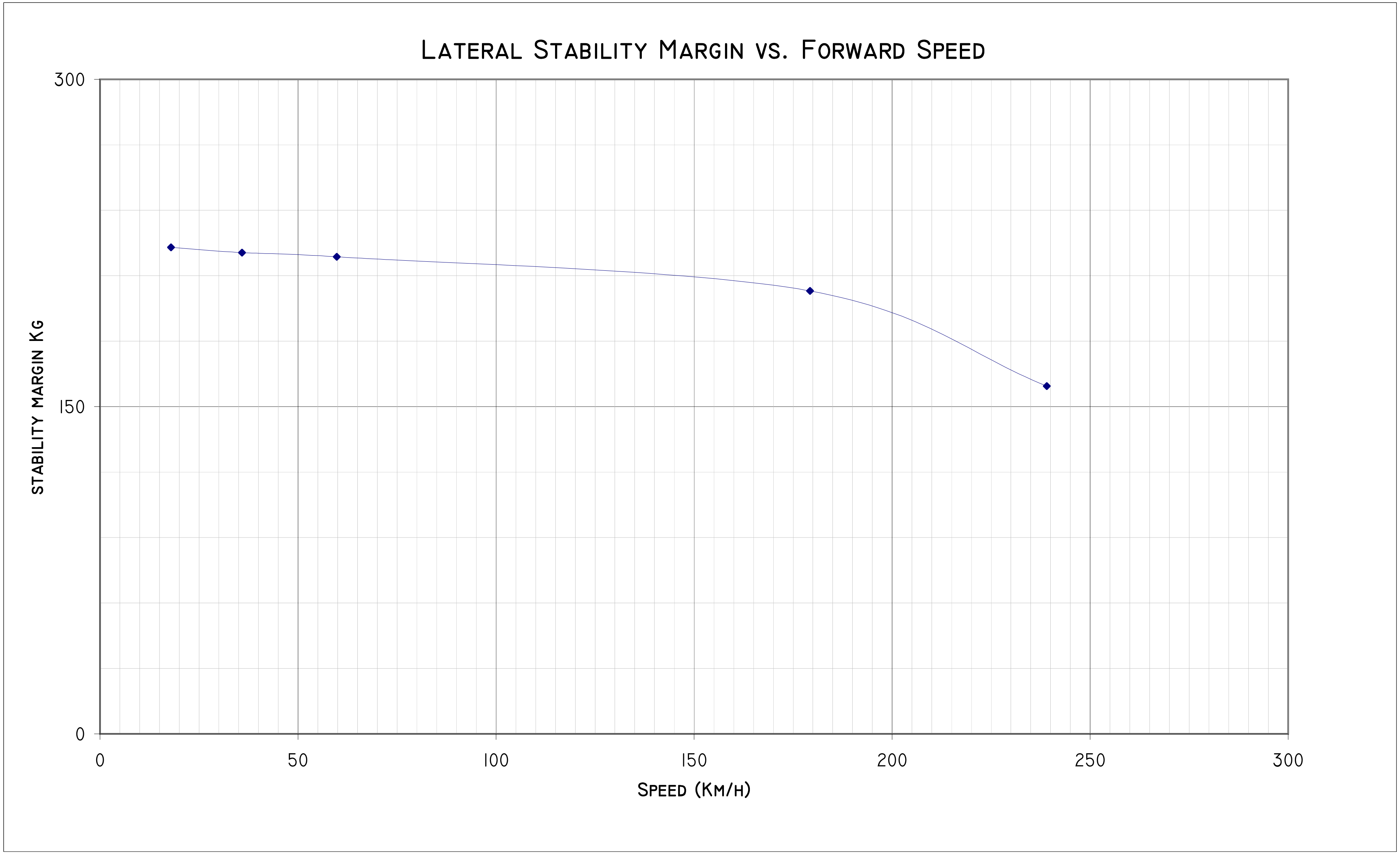

Lateral Stability Margin vs. Forward Speed
Stability margin Kg
300
150
0
Speed (Km/h)
0
50
100
150
200
250
300

APPENDIX E
CROSS FLOW

Fig. 1 E

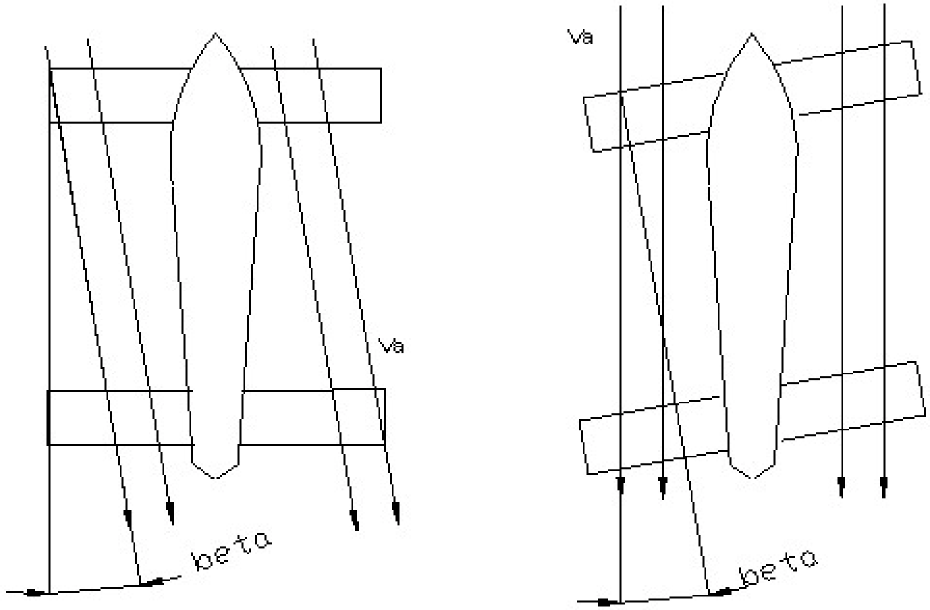

Fig. 2 E

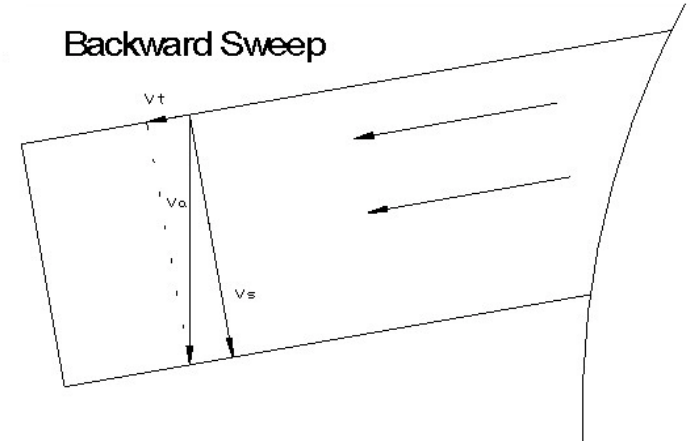

Fig. 3 E

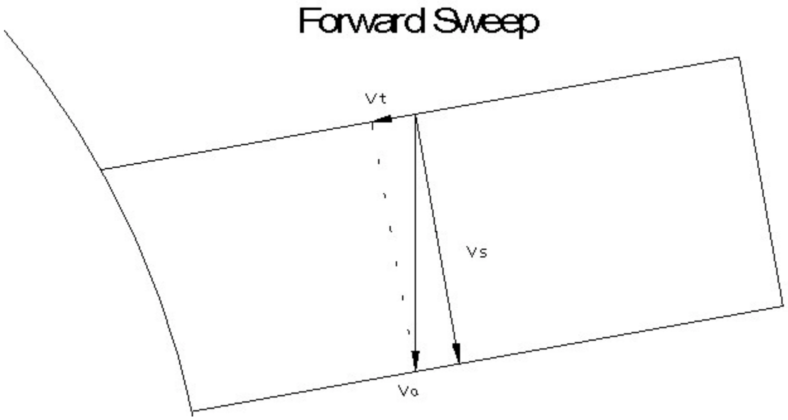

APPENDIX F
BODY DRAG

DRAG ANALYSIS FROM THE SIDE

SPEED (MACH NUMBER) DISTRIBUTION.

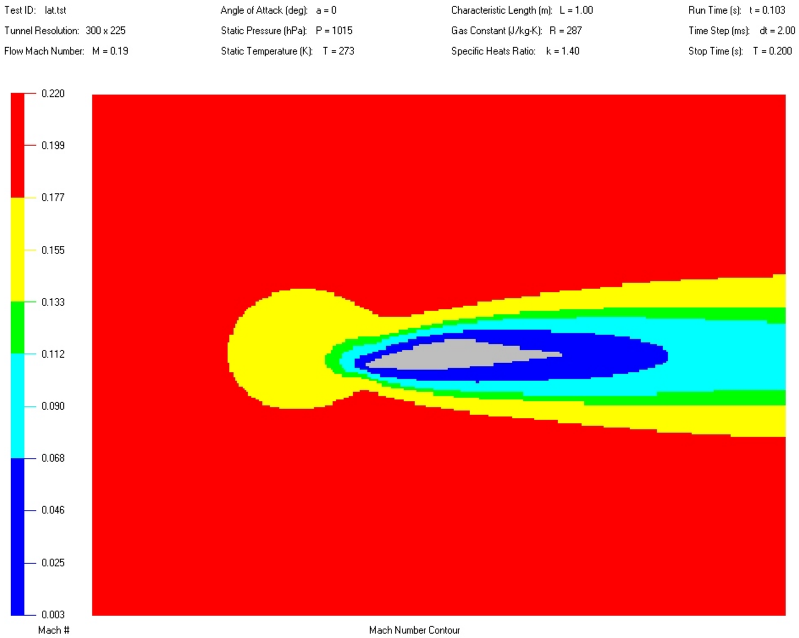

Fig. 1 F

PRESSURE DISTRIBUTION.

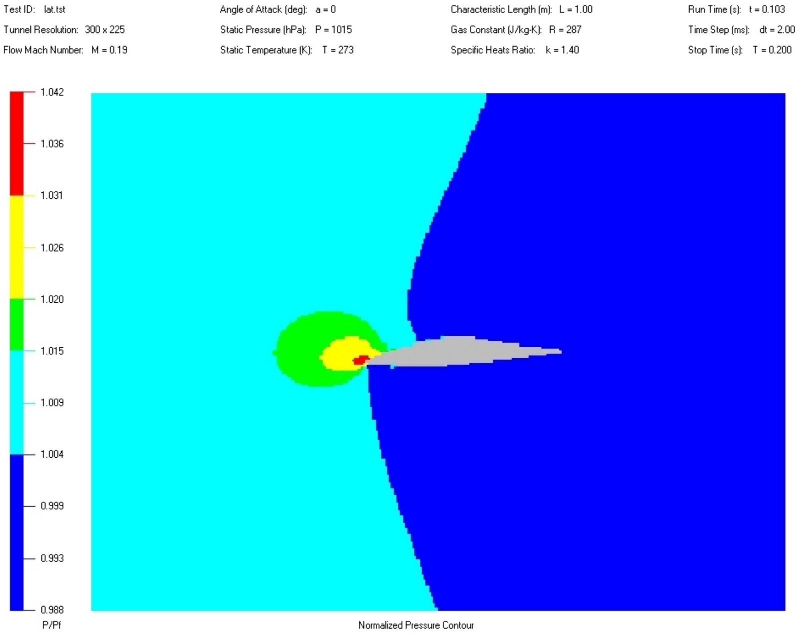

Fig. 2 F

STREAMLINES DISTRIBUTION.

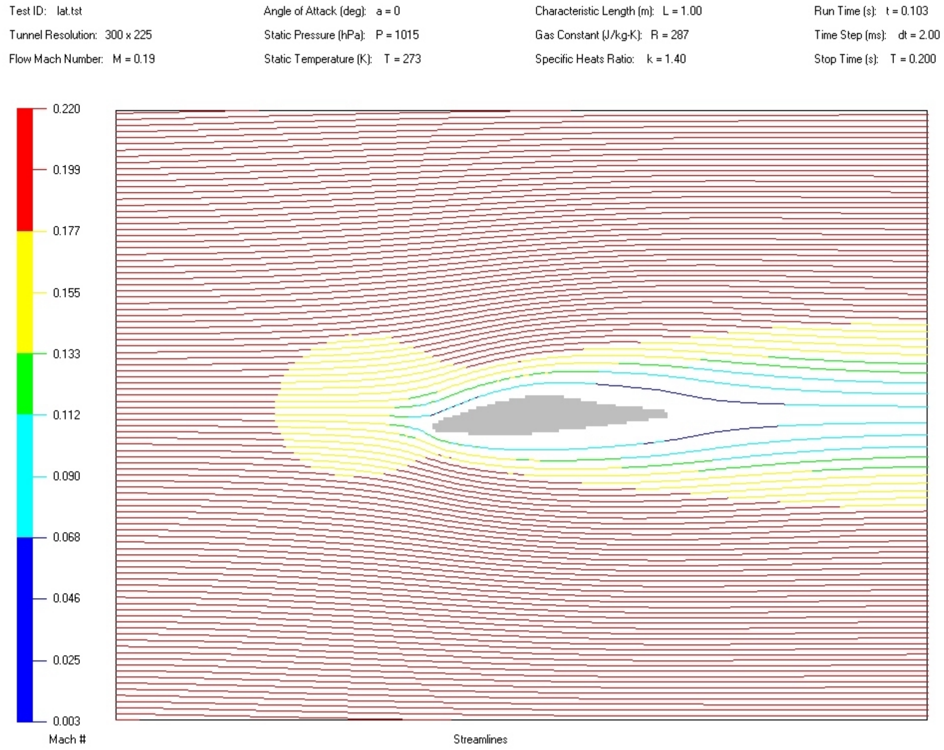

Test ID: lat.tst
Tunnel Resolution: 300 x 225
Flow Mach Number: M = 0.19

Angle of Attack (deg): a = 0
Static Pressure (hPa): P = 1015
Static Temperature (K): T = 273

Characteristic Length (m): L = 1.00
Gas Constant (J/kg-K): R = 287
Specific Heats Ratio: k = 1.40

Run Time (s): t = 0.103
Time Step (ms): dt = 2.00
Stop Time (s): T = 0.200

Fig. 3 F

STATISTICS
BODY 2D SIDE ANALYSIS

Test ID: b3.shp.tex

Tunnel Resolution: 300 x 225

Gas Constant (J/kg-K): R =287

Specific Heats Ratio: k =1.40

Mach Number:

Free Stream: M (inf) = 0.190

Maximum: M (max) = 0.220

Minimum: M (min) = 0.003

Pressure (hPa):

Free Stream: P (inf) = 1015

Maximum: P (max) = 1057

Minimum: P (min) = 1003

Temperature (K):

Free Stream: T (inf) = 273

Maximum: T (max) = 277

Minimum: T (min) = 273

Characteristic Length (m): L =1.00

Angle of Attack (deg): a =000

Section Coefficient of:

Lift: C (lift) =-0.210

Drag: C (drag) = 0.147

Moment: C (mom) = N/A

Density (kg/m^3):

Free Stream: Rh (inf) = 1.295

Maximum: Rh (max) = 1.330

Minimum: Rh (min) = 1.270

Speed of Sound (m/s):

Free Stream: a (inf) = 331

Maximum: a (max) = 334

Minimum: a (min) = 331

Table 1 F

DRAG ANALYSIS FROM THE TOP

SPEED (MACH NUMBER) DISTRIBUTION.

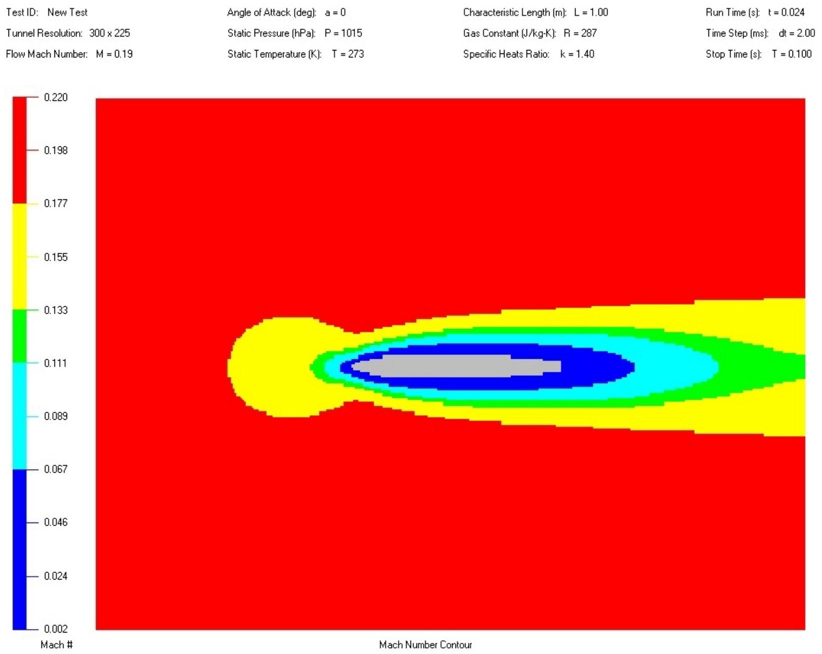

Test ID: New Test
Tunnel Resolution: 300 x 225
Flow Mach Number: M = 0.19
Angle of Attack (deg): a = 0
Static Pressure (hPa): P = 1015
Static Temperature (K): T = 273
Characteristic Length (m): L = 1.00
Gas Constant (J/kg-K): R = 287
Specific Heats Ratio: k = 1.40
Run Time (s): t = 0.024
Time Step (ms): dt = 2.00
Stop Time (s): T = 0.100

Fig. 4 F

PRESSURE DISTRIBUTION.

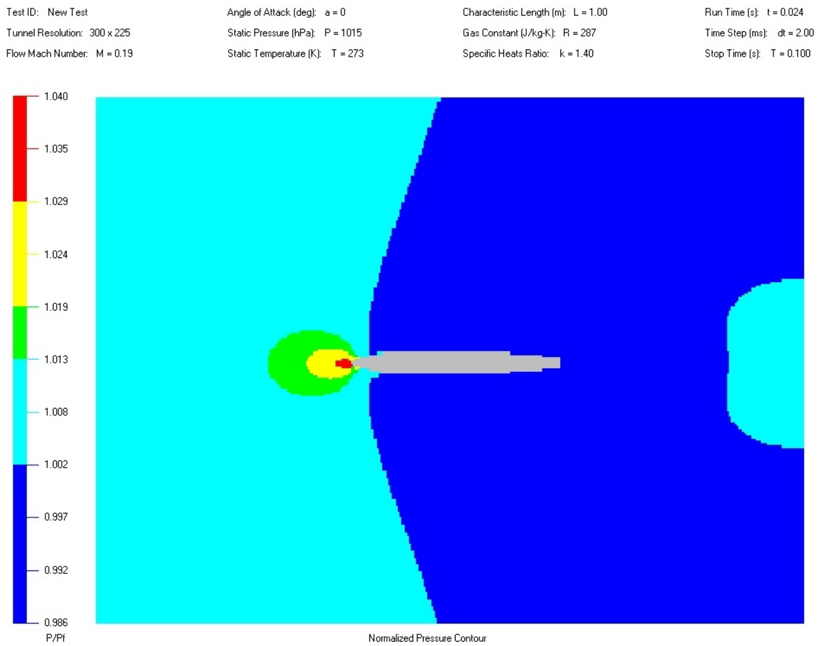

Test ID: New Test
Tunnel Resolution: 300 x 225
Flow Mach Number: M = 0.19
Angle of Attack (deg): a = 0
Static Pressure (hPa): P = 1015
Static Temperature (K): T = 273
Characteristic Length (m): L = 1.00
Gas Constant (J/kg-K): R = 287
Specific Heats Ratio: k = 1.40
Run Time (s): t = 0.024
Time Step (ms): dt = 2.00
Stop Time (s): T = 0.100

Fig. 5 F

STREAMLINES DISTRIBUTION.

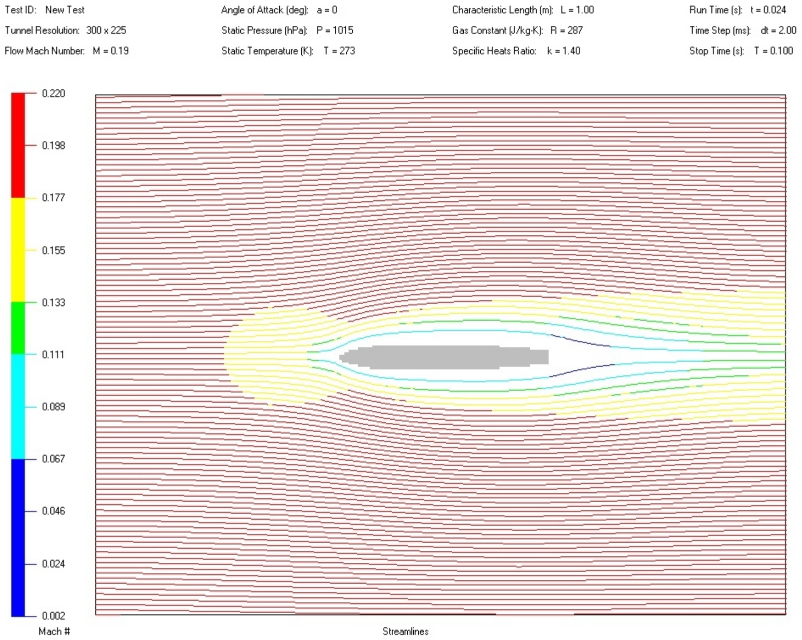

Test ID: New Test
Tunnel Resolution: 300 x 225
Flow Mach Number: M = 0.19
Angle of Attack (deg): a = 0
Static Pressure (hPa): P = 1015
Static Temperature (K): T = 273
Characteristic Length (m): L = 1.00
Gas Constant (J/kg-K): R = 287
Specific Heats Ratio: k = 1.40
Run Time (s): t = 0.024
Time Step (ms): dt = 2.00
Stop Time (s): T = 0.100

Fig. 6 F

STATISTICS
BODY 2D VIEW FROM THE TOP ANALYSIS

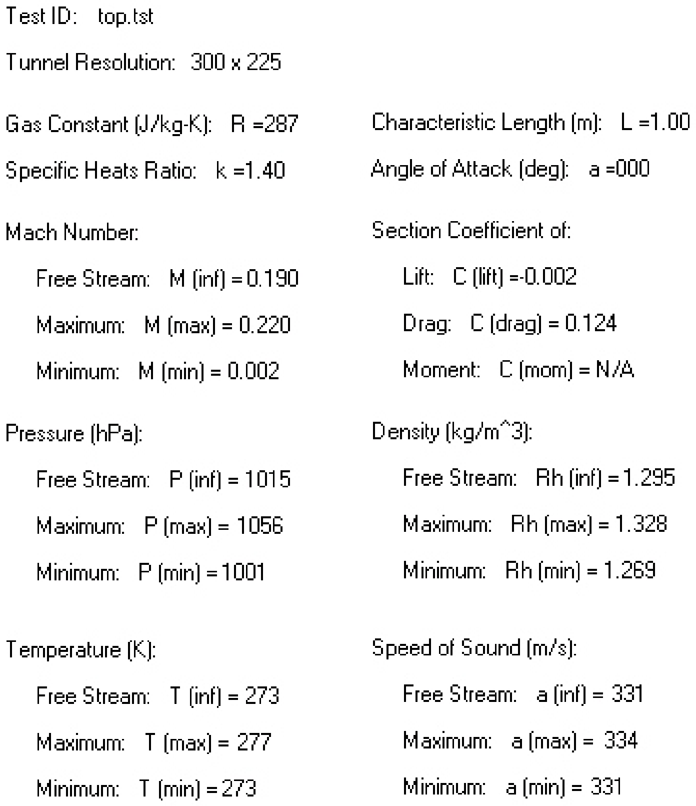

Test ID: top.tst

Tunnel Resolution: 300 x 225

Gas Constant (J/kg-K): R =287

Specific Heats Ratio: k =1.40

Characteristic Length (m): L =1.00

Angle of Attack (deg): a =000

Mach Number:

Free Stream: M (inf) = 0.190

Maximum: M (max) = 0.220

Minimum: M (min) = 0.002

Section Coefficient of:

Lift: C (lift) =-0.002

Drag: C (drag) = 0.124

Moment: C (mom) = N/A

Pressure (hPa):

Free Stream: P (inf) = 1015

Maximum: P (max) = 1056

Minimum: P (min) = 1001

Density (kg/m^3):

Free Stream: Rh (inf) = 1.295

Maximum: Rh (max) = 1.328

Minimum: Rh (min) = 1.269

Temperature (K):

Free Stream: T (inf) = 273

Maximum: T (max) = 277

Minimum: T (min) = 273

Speed of Sound (m/s):

Free Stream: a (inf) = 331

Maximum: a (max) = 334

Minimum: a (min) = 331

Table 2 F

APPENDIX G
HUMAN DIMENSIONS

Fig. 1 G

	PERCENTILE	
	3rd	99th
A Bideltoid breadth	427	514
B Biacromial breadth	370	452
C Hip breadth, sitting	332	415
D Stool height	376	471
E Thigh clearance height	137	191
F Acromial height, sitting	558	681

	PERCENTILE	
	3rd	99th
G Shoulder height, sitting	614	727
H Sitting eye height	765	896
J Sitting height	876	1007
K Vertical functional reach, sitting	1281	1515
L Knee Height, sitting	514	623

	PERCENTILE	
	3rd	99th
M Functional reach	736	889
N Cervicale height, sitting	627	745
O Elbow rest height, sitting	200	306
P Stomach depth	203	306
Q Buttock - knee length	558	672
R Buttock - heel length	998	1211

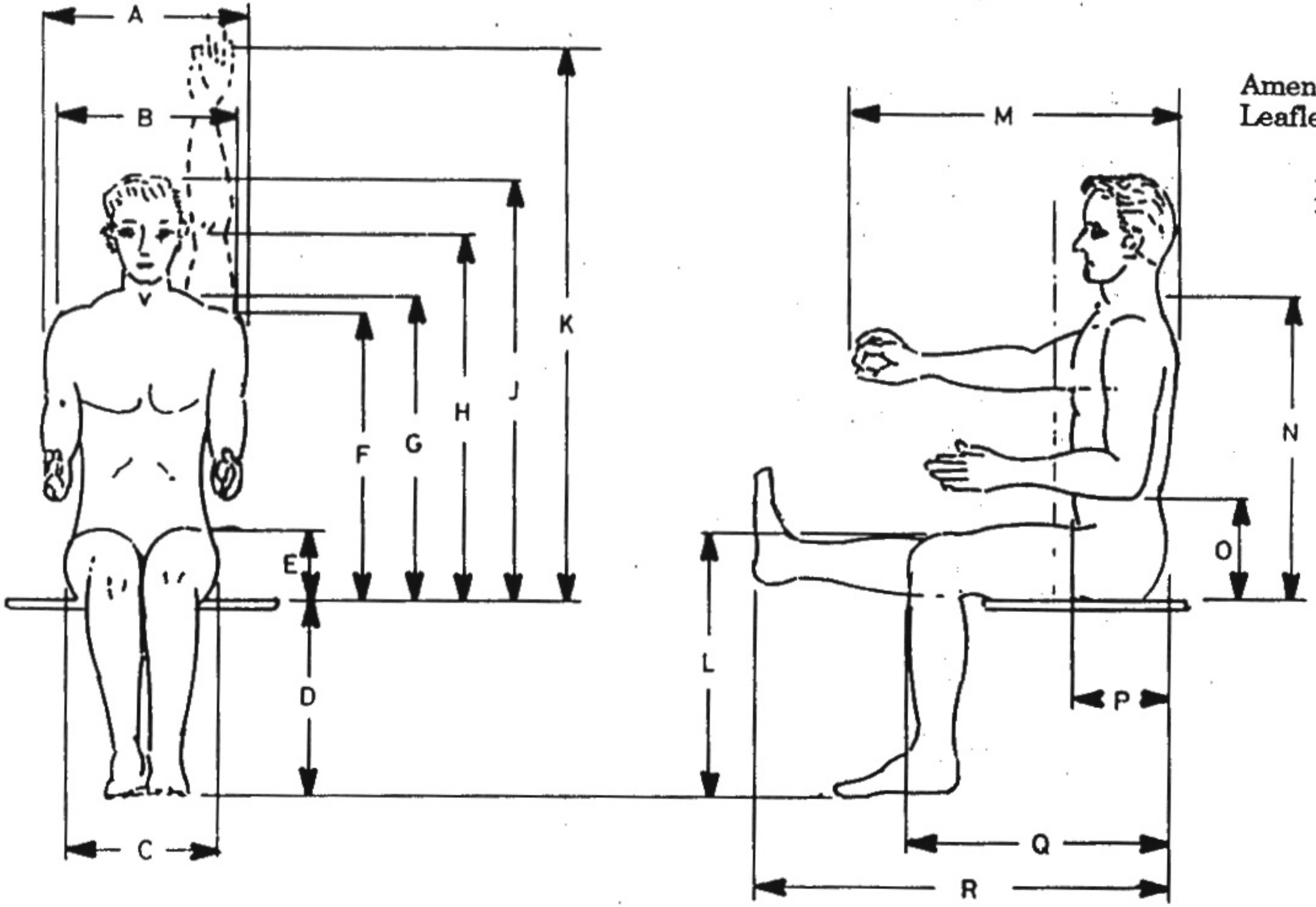

FIG. 1 RAF AIRCREW 3rd AND 99th PERCENTILE VALUES (mm)

Fig. 2 G

	PERCENTILE	
	3rd	99th
A Neck circumference	351	421
B Vertical trunk circumference (mean)	1504	1774
C Chest circumference	870	1111
D Waist circumference	720	1011
E Buttock circumference	895	1108
F Wrist circumference	157	197
G Thign circumference	496	659
H Calf circumference	327	416

	PERCENTILE	
	3rd	99th
I Ankle circumference	203	255
J Eye height, standing	1549	1808
K Axilla height	1238	1478
L Axilla - wrist length	424	544
M Crotch height	775	960
N Waist to waist over shoulder	817	982
O Crotch length	654	858
P Axilla - cervicale length	146	216
Q Axilla - fingertip length	607	749

	PERCENTILE	
	3rd	99th
R Fingertip height	606	749
S Cervicale - crotch length	612	727
T Shoulder height, standing	1396	1646
U Cervicale - vertex length	231	293
V Cervicale - waist length	355	443
W Waist height	1023	1227
X Cervicale height	1410	1661
Y Stature	1661	1924

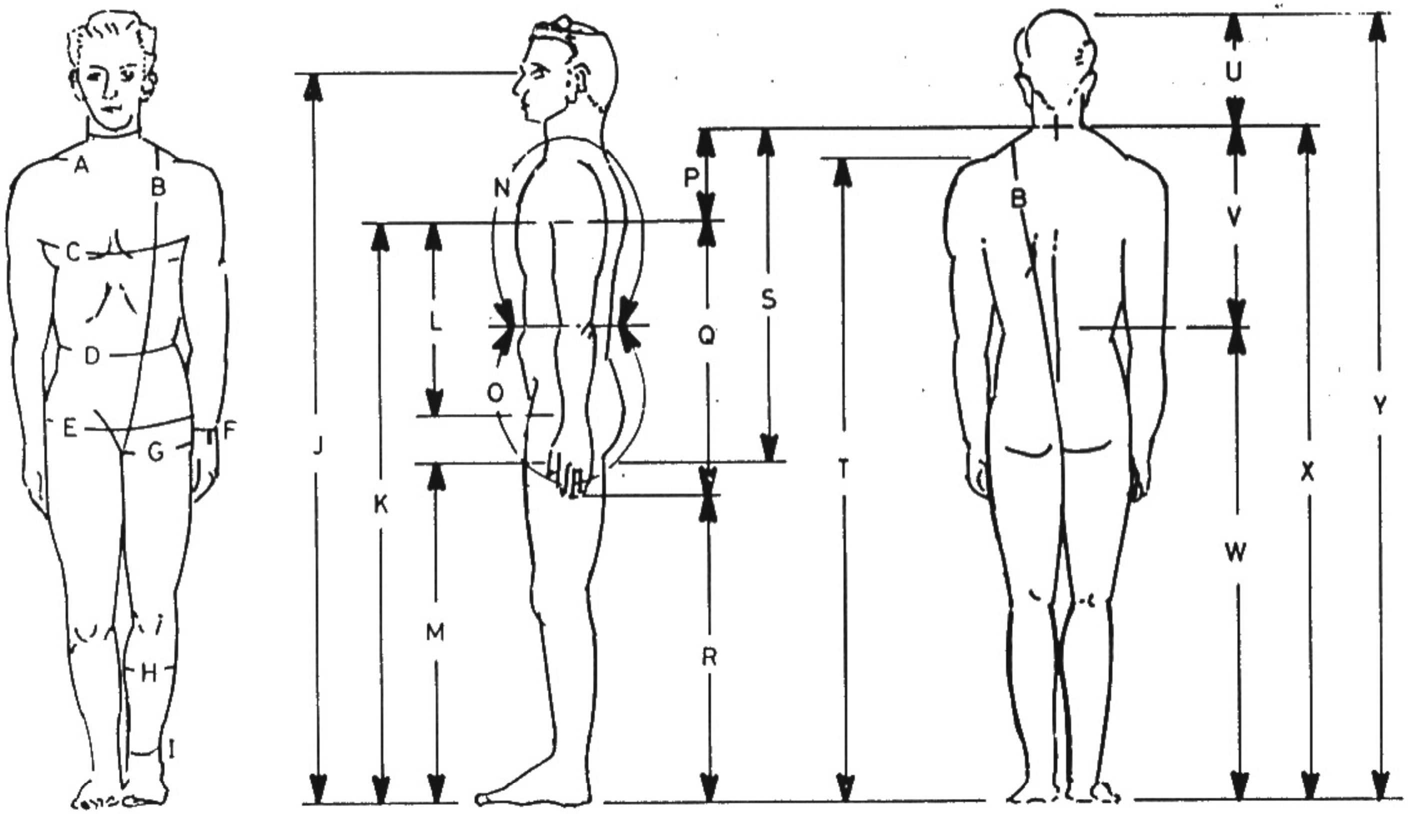

FIG.2 RAF AIRCREW 3rd AND 99th PERCENTILE VALUES (mm)

Fig. 3 G

		PERCENTILE	
		3rd	99th
A	Span	1692	2014
B	Inter-elbow span	909	1088
C	Elbow-fingertip length	442	531
D	Elbow-wrist length	261	323
E	Hand length	173	216
F	Elbow-functional reach	384	464

		PERCENTILE	
		3rd	99th
G	Elbow, fully bent, circumference	310	384
H	Knee, fully bent, circumference	406	495
J	Foot breadth	87	106
K	Ball of foot circumference	228	278
L	Instep-sole circumference	228	273
M	Foot length	244	297
N	Heel-instep circumference	300	359

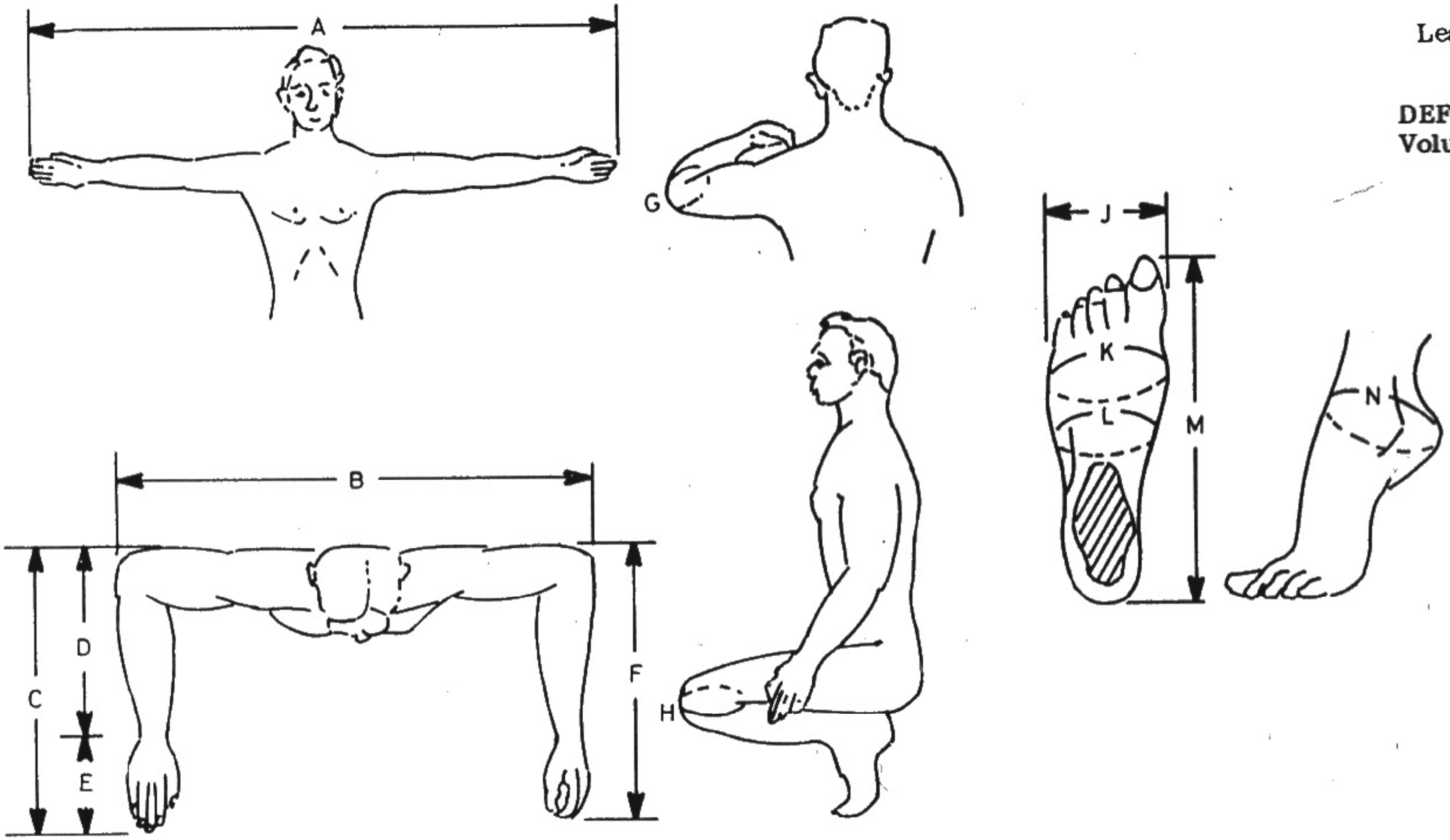

FIG.3 RAF AIRCREW 3rd AND 99th PERCENTILE VALUES (mm)

APPENDIX H

OVERALL DRAG

DRAG ESTIMATION

Table 1 H

SPEED (KM/H)	DRAG COMPONENTS					
	SAIL (N)	WINGS (N)	BODY (N)	PARASITE (N)	TOTAL (N)	THRUST (N)
17.9305	6.8	3.731615	0.861846	0.998183	12.3322	199
35.861	18.04	15.02702	3.447578	1.786382	38.20987	273.3
59.76834	43	40.67193	9.576606	3.654672	97.72578	390
179.305	351	372.4386	86.18463	27.00683	839.3305	1076
239.0734	622	695.0327	153.1317	47.41406	1489.514	1466

Fig. 1 H

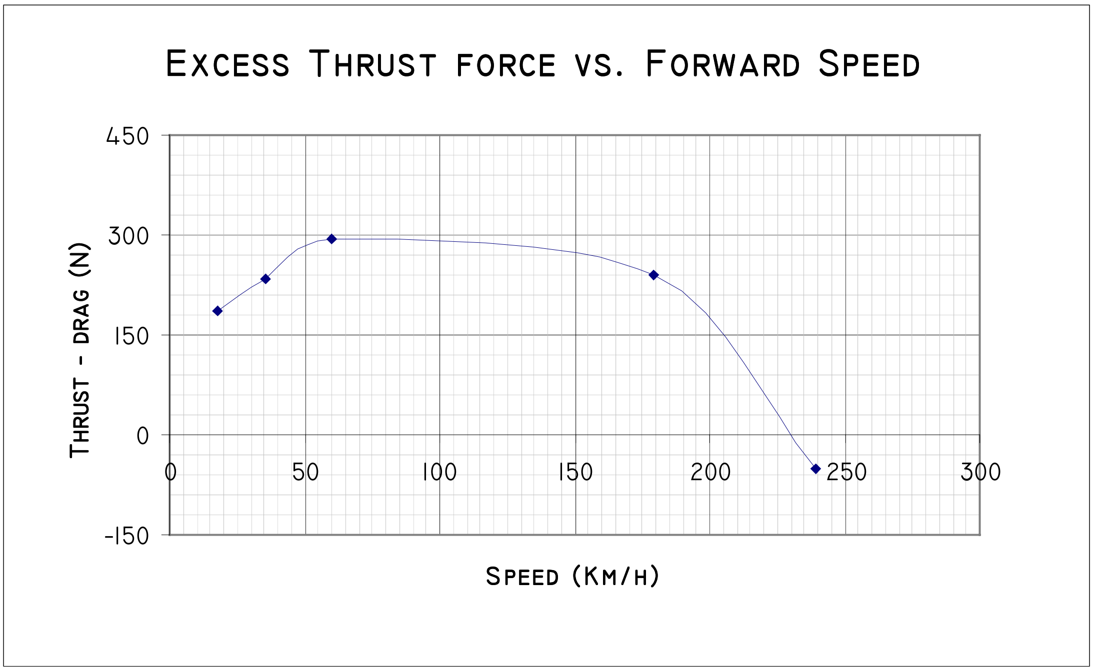

APPENDIX I
FINAL CONFIGURATION.

SUMMARY OF RESULTS

ENVIRONMENTAL CONDITIONS

Temperature = 0°C

Viscosity = 1.72e-5

Density = 1.293 Kg/m^3

True wind = 8.3 m/s

PERFORMANCE

Maximum speed with true wind of 8.3 m/s is 231.3 Km/h

MAIN SAIL[1]

Airfoil section = Wortmann FX-63 137
AR =6.2
Cord at tip = 0.62 m
Cord at root = 1.38 m
Taper ratio = 0.45

SPEED (KM/H)	17.93	35.86	59.76	179.30	239.07
FORWARD FORCE (N)	199	273.3	390	1076	1466
DRAG (N)	6.8	18.04	43	351	622

WINGS

Number = 2 (complete wings)
Airfoil Section = NACA 63(1)412
Distance to the floor (closest point)= 0.1 m
AR = 5
Span (runner to runner) = 3.5 m
Incidence = 4°

SPEED (KM/H)	17.93	35.86	59.76	179.30	239.07
CL.(CORRECTED FOR AR)	-0.77	-0.79	-0.78	-0.79	-0.79
DOWN FORCE (N)	-61.20	-61.20	-61.20	-61.20	-61.20
DRAG (N)	3.73	3.73	3.73	3.73	3.73

BODY

Cl at 239Km/h = - 0.210

Cd at 239Km/h = 0.1355

STEERING SYSTEM

Parallel steering system with dampers and centering springs.

FRONT SUSPENSION

Dampers and coil spring shock absorbers.

Mounted on tip of the wings.

---

[1] Details about the wing can be found in Mr. de Valence report.

APPENDIX J
DRAWINGS.

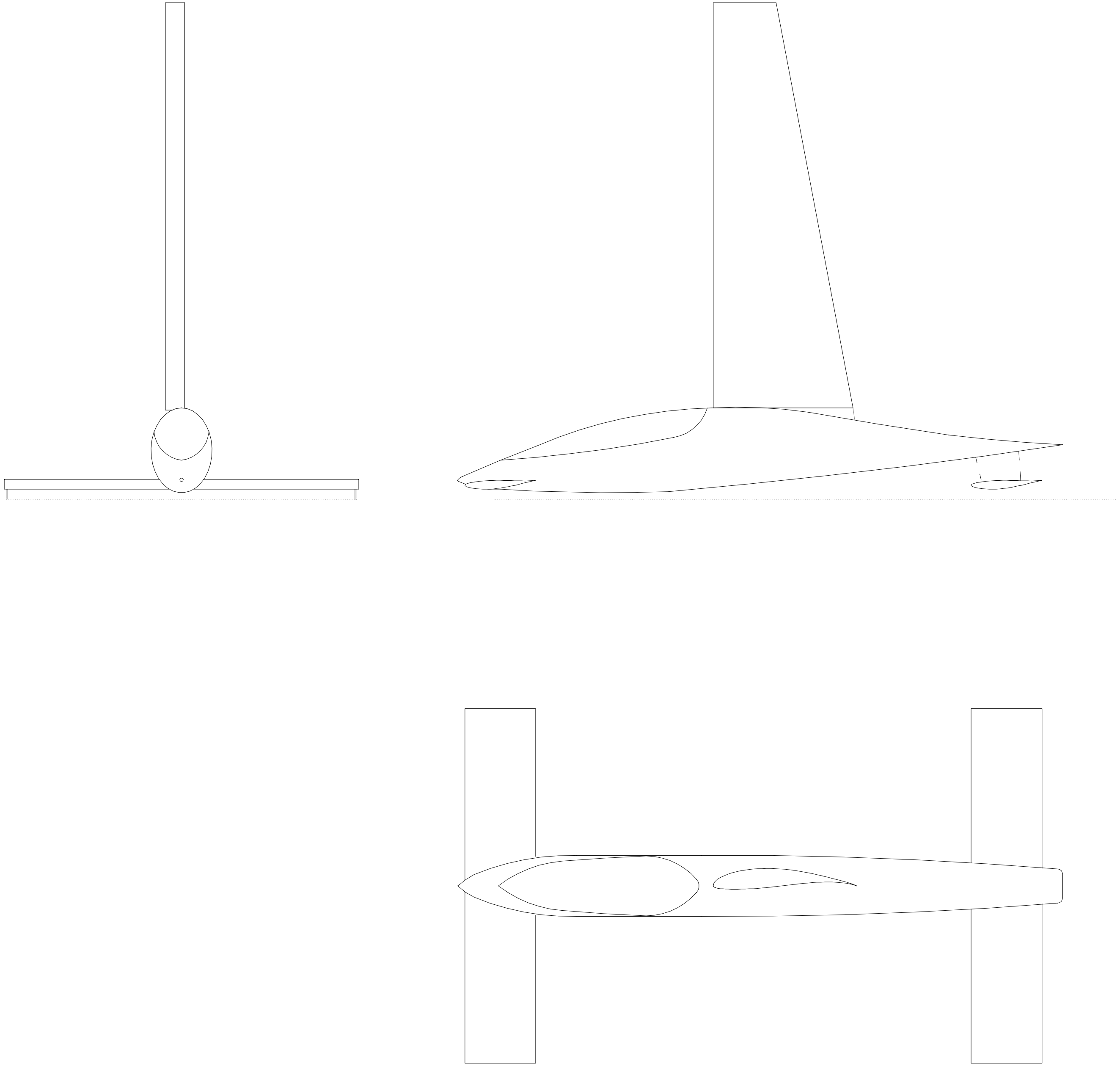

FEBRUARY 2000 ICE YACHT

JAVIER CUADRIELLO RODRIGUEZ

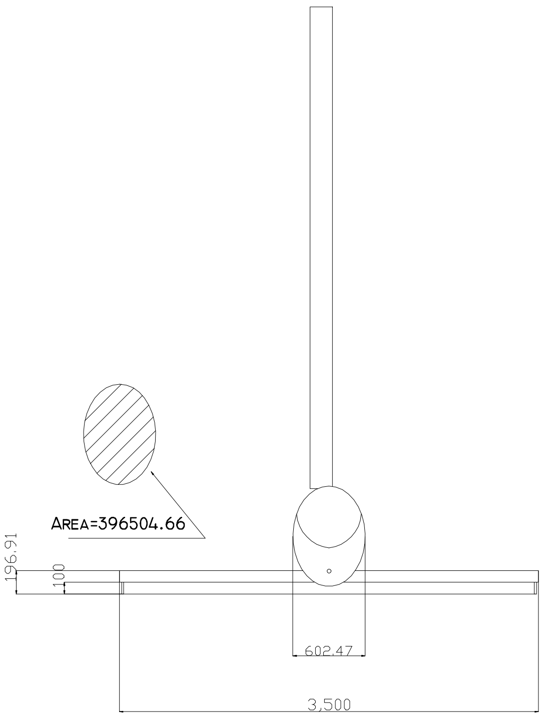

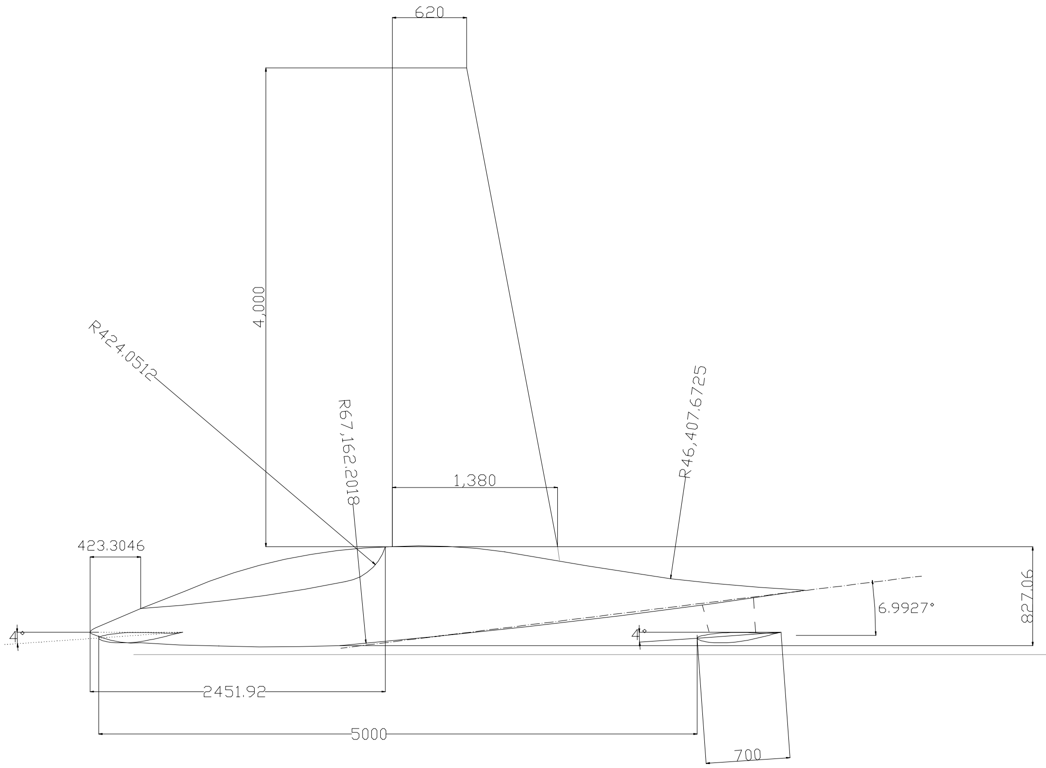

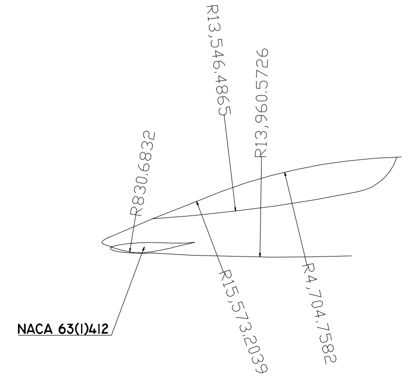

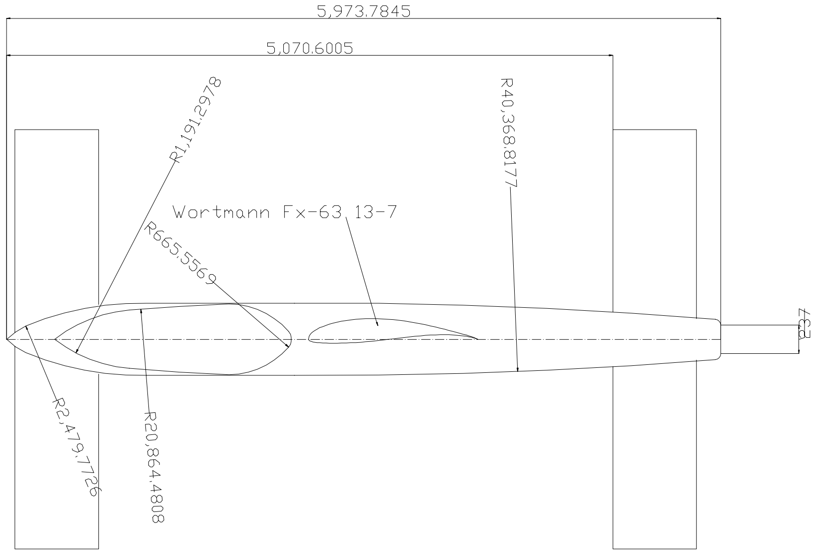

FEBRUARY 2000 ICE YACHT

JAVIER CUADRIELLO RODRIGUEZ

PILOT'S REACH

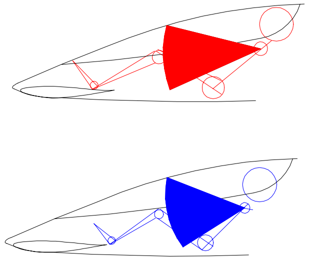

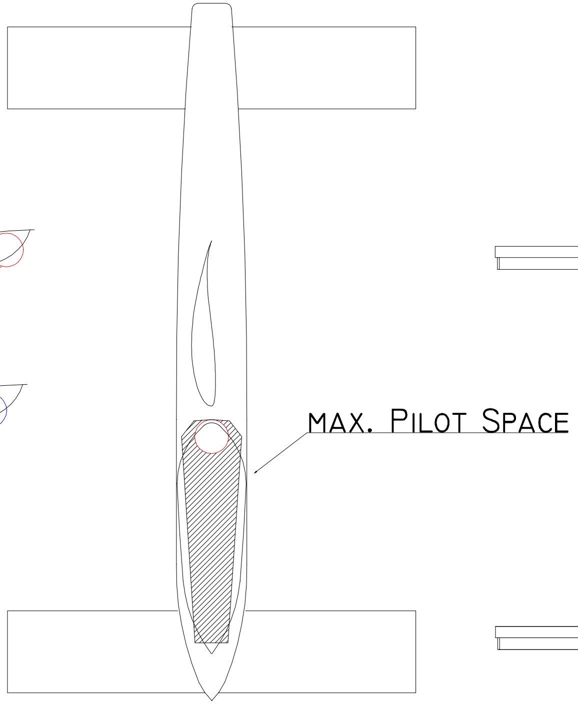

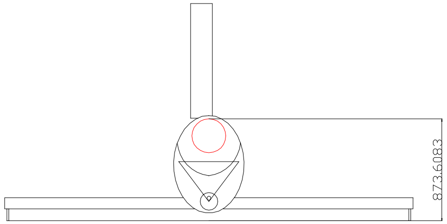

BIGGEST PILOT

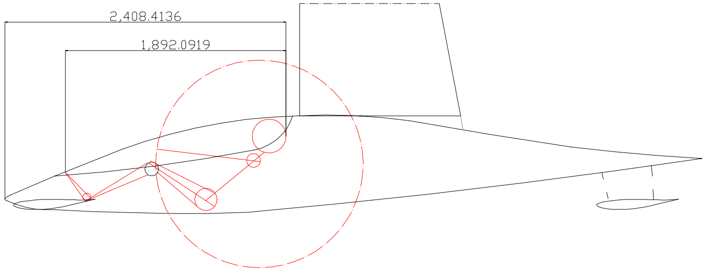

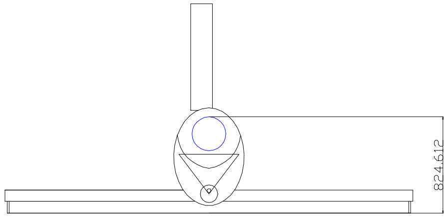

SMALLEST PILOT

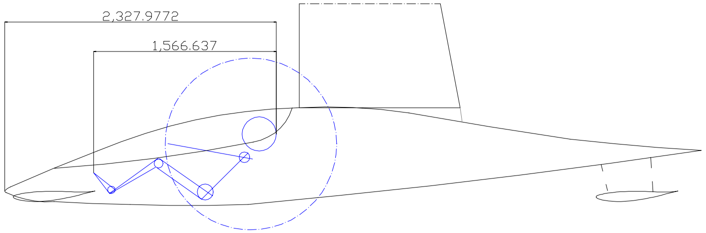

FEBRUARY 2000

ICE YACHT - PILOT SIZES

JAVIER CUADRIELLO RODRIGUEZ

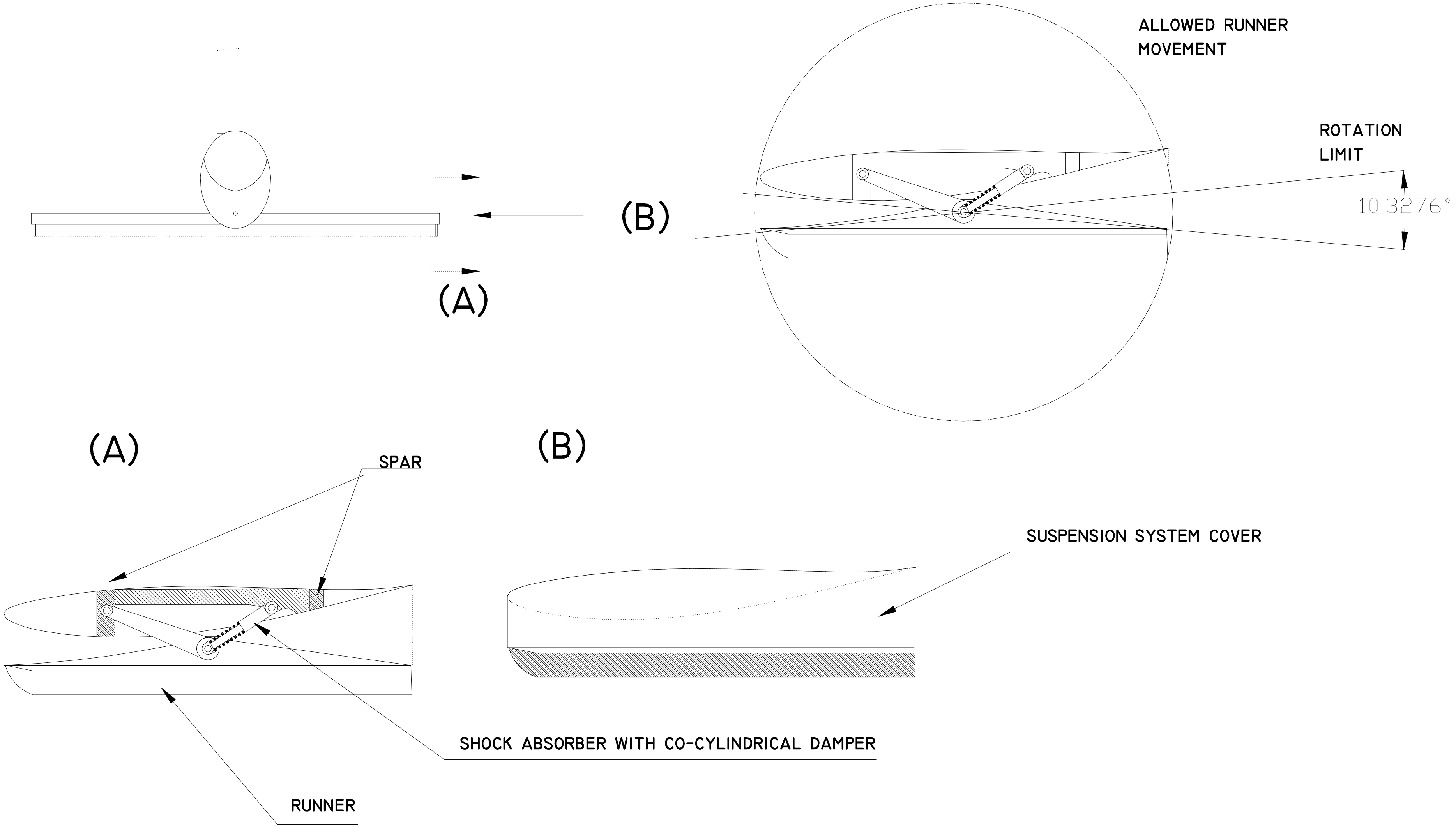

FEBRUARY 2000 SUSPENSION

JAVIER CUADRIELLO RODRIGUEZ

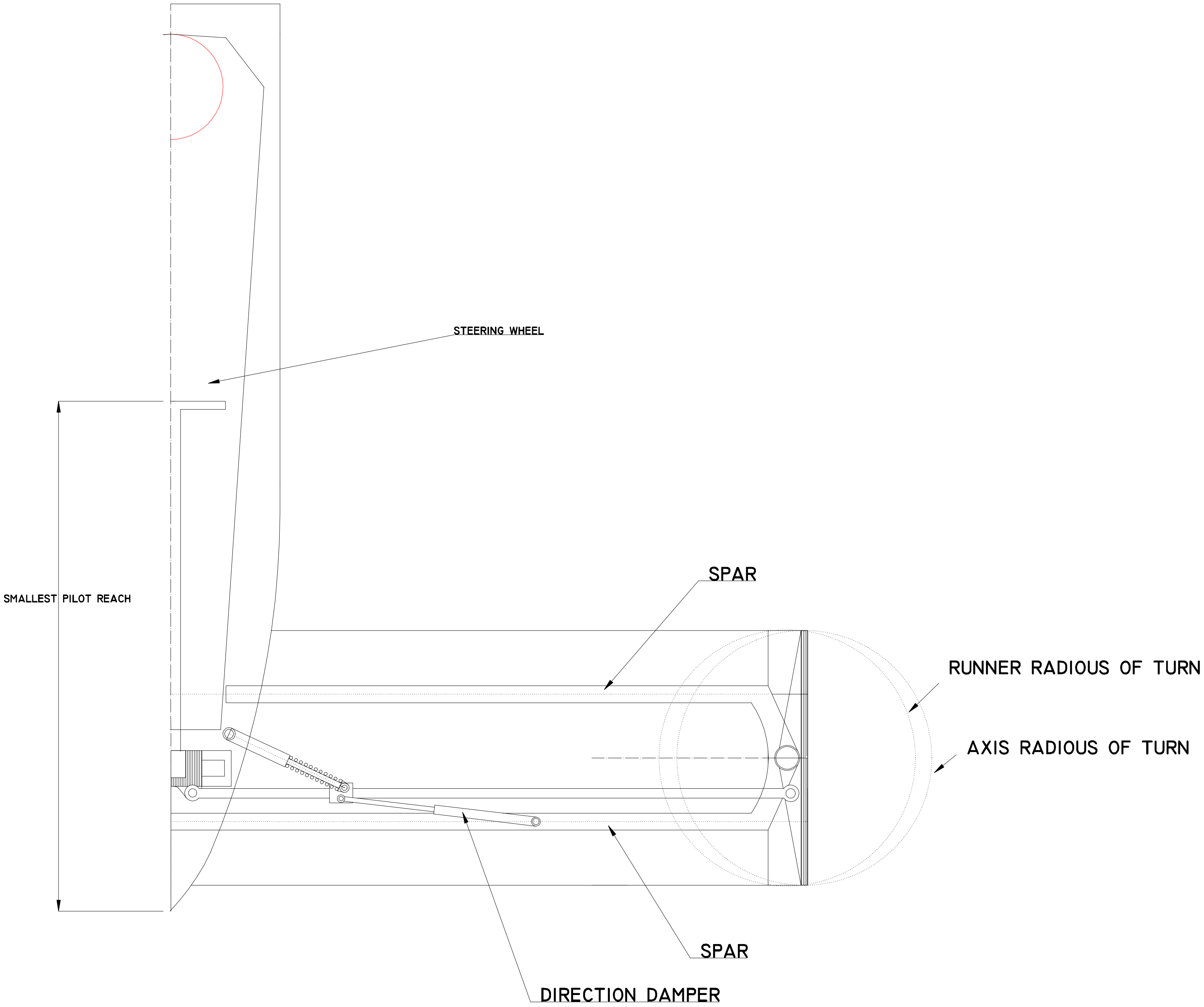

FEBRUARY 2000

DIRECTION

JAVIER CUADRIELLO RODRIGUEZ